Electron Paramagnetic Resonance of Gd^{3+} Pairs in Rare-Earth Hydroxides*

R. W. Cochrane,† C. Y. Wu,‡ and W. P. Wolf
Department of Engineering and Applied Science, Becton Center, Yale University, New Haven, Connecticut 06520
(Received 21 May 1973)

Electron paramagnetic resonance has been observed from isolated nearest-neighbor (nn) and next-nearest-neighbor (nnn) pairs of Gd^{3+} in $Y(OH)_3$ and $Eu(OH)_3$ at 77 K and 23 GHz. The spectra were analyzed in the same way as previous measurements on Gd^{3+} pairs in $LaCl_3$ and $EuCl_3$ and, as before, the dominant interactions were found to be isotropic bilinear exchange ($J\mathbf{S}_1 \cdot \mathbf{S}_2$) and magnetic dipole coupling, with small crystal-field terms. However, the relative strengths of the interactions turned out to be rather different, and in the case of the nearest neighbors this gave rise to some interesting complications. It was found that all of the observable lines (about 40 in each case) were almost equally sensitive to bilinear and biquadratic isotropic interactions, with the result that only the combination $J'_{nn} = J_{nn} - 41Q_{nn}$ could be determined accurately, where Q_{nn} is the coefficient of the biquadratic coupling expressed in the form $Q_{nn}\sum_{m=2}^{m=-2}(-1)^m O_m^{(2)}(S_1)O_{-m}^{(2)}(S_2)$. For the next-nearest-neighbor pairs no such complication was evident and a unique fit was obtained with $Q_{nnn} = 0$. J'_{nn} and J_{nnn} were fitted to the observed spectra and the following values were obtained: $J'_{nn}[Y(OH)_3] = 0.164 \pm 0.006$ cm^{-1}, $J_{nnn}[Y(OH)_3] = -0.0060 \pm 0.0001$ cm^{-1}; and $J'_{nn}[Eu(OH)_3] = 0.134 \pm 0.007$ cm^{-1} and $J_{nnn}[Eu(OH)_3] = -0.0146 \pm 0.0001$ cm^{-1}. Comparison with an independent analysis of magnetic-susceptibility and specific-heat data for concentrated $Gd(OH)_3$ indicated excellent agreement if $Q_{nn} \ll J_{nn}$, and an upper limit $|Q_{nn}| \lesssim 5 \times 10^{-4}$ cm^{-1} was estimated. However, further detailed study showed that there are additional *anisotropic* biquadratic terms which are not entirely negligible and that the nearest-neighbor spectra could be fitted adequately only if three small terms of the form $q^{|m|}O_m^{(2)}(S_1)O_{-m}^{(2)}(S_2)$ with $m = \pm 2, \pm 1$, and 0 were included in the interactions. The fitted coefficients $q^{|m|}$ were all in the range of 10^{-4} cm^{-1}, which is much larger than one might have guessed for such high-order terms. However, more detailed estimates by Cone have recently shown that both the relative and the absolute magnitudes of the $q^{|m|}$ can in fact be explained in terms of the measured excited-state exchange interactions in $Gd(OH)_3$ and $GdCl_3$ and the known spin-orbit admixtures of ^6P into the ^8S ground state. These results suggest that biquadratic interactions could be larger than is generally assumed also in other cases, although their effects will usually be observable only in detailed spectroscopic experiments. There is at present no microscopic explanation for the much larger bilinear exchange parameters, J_{nn} and J_{nnn} or even their signs, but the values found are consistent with a recent empirical correlation between J's in different gadolinium compounds. This suggests that the dominant exchange mechanism in these systems involves only the Gd^{3+} ions and not, as in the more usual superexchange interaction, the intermediate ligands.

I. INTRODUCTION

The rare-earth hydroxides, $R(OH)_3$ with R = La to Yb and Y, crystallize as simple hexagonal lattices which are isostructural with the light rare-earth trichlorides, tribromides, and ethyl sulphates. Of these materials, the hydroxides have the most compact lattices, with lattice parameters about 14% smaller than the trichlorides, and we might therefore expect the strongest magnetic interactions. Recent measurements in our laboratory[1,2] have indicated that the hydroxides do indeed exhibit interesting magnetic properties at readily accessible temperatures, but many of these properties are strikingly different from those observed in the corresponding trichlorides, in spite of the general similarity between the crystals. The comparison between $Gd(OH)_3$ and $GdCl_3$ furnishes just such an example: $Gd(OH)_3$ is found to order antiferromagnetically[2] at 0.94 K, whereas $GdCl_3$ undergoes a ferromagnetic transition at 2.2 K.[3] This surprising difference in both the magnitudes and signs of the dominant interactions has provided the motivation for the present detailed study of Gd^{3+}-Gd^{3+} pair interactions in various hydroxide lattices.

In this paper we report electron-spin-resonance measurements on isolated pairs of Gd^{3+} nearest neighbors (nn) and next nearest neighbors (nnn) in the hosts $Y(OH)_3$ and $Eu(OH)_3$, and an analysis in terms of the appropriate spin Hamiltonian. Of these hosts $Y(OH)_3$ is diamagnetic and $Eu(OH)_3$ is only weakly magnetic, owing to the first excited state $^7F_1$ about 350 cm^{-1} above the ground state, $^7F_0$. At low temperatures (liquid nitrogen and below) the first excited state is not appreciably populated and its only effect is to allow small admixtures into the nonmagnetic ground state. These are observed as small g shifts in both the single-ion and pair resonance spectra, which may be used to provide additional information about Gd^{3+}-Eu^{3+} interactions.

Both $Y(OH)_3$ and $Eu(OH)_3$ are excellent matrices for comparing the Gd^{3+} pair interaction with those for $Gd(OH)_3$, since these lattices are isostructural, with lattice dimensions which closely bracket those for the concentrated $Gd(OH)_3$. $La(OH)_3$ is also a

diamagnetic member of this series, and as such would be another ideal system in which to study pair interactions. Unfortunately, single crystals of adequate size have not yet been produced, but hopefully some will be available in the near future.

The spin resonance of an isolated pair of magnetic ions in a nonmagnetic insulating host has been discussed in detail by Hutchings *et al.*[4,5] (hereafter referred to as I and II), who analyzed, in particular, the regime of comparable isotropic and anisotropic interactions which is appropriate for most rare-earth insulators. The specific application was to the study of Gd^{3+} pair interactions in $LaCl_3$ and $EuCl_3$, and in the present investigation we shall rely heavily on the experience derived from the trichloride experiments. We shall find results generally similar to those for the trichlorides, with the dominant interactions closely described by an isotropic bilinear exchange and a dipole-dipole coupling. However, there were two surprising features in the present results which are of particular interest for understanding the spin-spin interactions between Gd^{3+} ions in systems of this kind.

First, it was found necessary to include small but definitely nonzero higher-order biquadratic interactions into the pair Hamiltonian to describe the observed pair spectra for the nearest neighbors. Such terms had not been found to be significant in the earlier study of the trichlorides. Moreover, the required form for this interaction turned out to be *anisotropic* with axial symmetry about the bond axis, in contrast to the more usual isotropic biquadratic exchange. In the present experiments, the isotropic biquadratic terms cannot be separated unambiguously from the isotropic bilinear term, but a comparison with magnetic and thermal results for bulk $Gd(OH)_3$[6] indicates that the isotropic biquadratic exchange must be quite small.

Second, a comparison of the nearest- and next-nearest-neighbor exchange parameters for the hydroxides with those previously obtained for the chlorides and several other crystals[7] reveals a simple linear trend with ionic separation, including interactions which are both ferromagnetic and antiferromagnetic in sign. This surprising result provides at least an empirical explanation for the marked differences in magnetic order between $Gd(OH)_3$ and $GdCl_3$ referred to earlier.

In Sec. II we shall review the spin Hamiltonian for an isolated pair of Gd^{3+} ions and the features of the EPR pair spectra arising from this Hamiltonian. The details of the hydroxide samples and the experimental apparatus are discussed in Sec. III. The next three sections present the experimental results (Sec. IV), a general outline of the fitting procedure (Sec. V), and the interpretation of the pair spectra (Sec. VI). The interaction parameters so derived are discussed in Sec. VII, which includes also a comparison with the previous results for Gd^{3+} pairs in the trichloride hosts.

II. SPIN HAMILTONIAN

The spin Hamiltonian appropriate to a pair of Gd^{3+} ions can generally be written in the form[4]

$$\begin{aligned}\mathcal{H}(1,2) = {} & g\mu_B \vec{H}\cdot(\vec{S}_1+\vec{S}_2) \\ & + J\vec{S}_1\cdot\vec{S}_2 + \alpha(\vec{S}_1\cdot\vec{S}_2 - 3S_{z1}S_{z2}) \\ & + V_c(1) + V_c(2) \\ & + \mathcal{H}_{\rm int}^{(1)}\,, \end{aligned} \tag{1}$$

where the pair axis has been labeled as the z axis. In this expression the first term is the usual Zeeman energy with g taken to be isotropic, the next two are the isotropic exchange and magnetic dipole interactions (with $\alpha = g^2\mu_B^2/r_{12}^3$), and $V_c(i)$ is the crystal field acting on the ith site. The final term $\mathcal{H}_{\rm int}^{(1)}$ represents all other possible higher-order interaction effects, which we would expect to be very small, as in previously studied situations. Neglecting $\mathcal{H}_{\rm int}^{(1)}$ for the present and considering only fields applied along the z axis, we can simplify Eq. (1) and write an approximate zero-order Hamiltonian

$$\begin{aligned}\mathcal{H}^{(0)}(1,2) = {} & g\mu_B H(S_{z1}+S_{z2}) \\ & + J\vec{S}_1\cdot\vec{S}_2 + \alpha(\vec{S}_1\cdot\vec{S}_2 - 3S_{z1}S_{z2}) \\ & + \sum_{i=1,2} \tfrac{1}{3}b_2^0 O_2^0(i) + \tfrac{1}{60}b_4^0 O_4^0(i) + \tfrac{1}{1260}b_6^0 O_6^0(i), \end{aligned} \tag{2}$$

where the crystal field terms have been written in the usual form,[4,8] retaining only those terms which will give a first-order contribution to the line positions.

The main characteristics of the resonance spectrum corresponding to Eq. (2) have been described in I. For $H=0$, the energy levels of $\mathcal{H}^{(0)}$ (1, 2) are eigenvalues of $|T_z|$, where $\vec{T} = \vec{S}_1 + \vec{S}_2$ is the total spin of the pair, and each state is twofold degenerate. For nonzero fields applied along the c axis, T_z remains a good quantum number and the energy levels diverge linearly. The spectrum should therefore consist of pairs of equally intense lines situated symmetrically about the central transition at $H_0 = h\nu/g\mu_B$, with field splittings $\Delta H = |H - H_0|$ which are *independent* of the microwave frequency ν. When the magnetic field is rotated away from the pair bond axis by a small amount, the resonant fields should turn symmetrically about this axis, with either a maximum or a minimum along the axis. These three characteristics identify a transition as part of the pair spectrum belonging to a particular set of neighboring ions, and it is these features which are used to identify and classify experimentally observed resonance lines as pair transitions.

In general the behavior predicted by Eq. (2) was followed quite accurately by all the observed lines, and in particular the symmetry about H_0 was found for all pairs of lines with good precision. This indicates that any of the possible terms in $\mathcal{H}_{\text{int}}^{(1)}$ which we have neglected so far must commute with T_z, as one might expect if one regards the pair bond as having predominantly axial symmetry.

Anticipating the fact that we shall not be able to fit the observed spectra completely with the terms given in Eq. (2), we can consider phenomenologically possible higher-order terms which would satisfy the requirement of commuting with T_z. If we consider all the allowed biquadratic terms, [9] we find that they can be characterized by three parameters, $Q^{|m|}$ $(m=0, 1, 2)$, for each type of pair:

$$\mathcal{H}_Q(1,2)=\sum_{m=2}^{-2} Q^{|m|}(1,2)\,O_m^{(2)}(1)\,O_{-m}^{(2)}(2), \tag{3}$$

where we have used normalized spherical tensor operators as defined by Smith and Thornley. [10,11] This expression could of course also be written in terms of more conventional products of spin operators, such as $(\vec{S}_1\cdot\vec{S}_2)^2$ and $S_{z1}^2 S_{z2}^2$, but the irreducible tensor form would seem to offer a more direct link to possible physical mechanisms. We shall discuss some of these in Sec. VII A in the light of the experimentally observed values of the Q's.

The general biquadratic expression in Eq. (3) can be decomposed into a scalar part [12]

$$\mathcal{H}_{QS}(1,2)=Q\sum_{m=2}^{-2}(-1)^m O_m^{(2)}(1)\,O_{-m}^{(2)}(2), \tag{4}$$

and a residual anisotropic part with coefficients

$$q^{|m|}=Q^{|m|}-(-1)^m Q, \tag{5}$$

where

$$Q=(2Q^{|2|}-2Q^{|1|}+Q^0)/5. \tag{6}$$

We shall see that the analysis of the experimental results is not very sensitive to the scalar part Q in the present cases, so that only the anisotropic coefficients $q^{|m|}$ can be determined with certainty. The isotropic term Q appears strongly correlated with the isotropic *bilinear* exchange coefficient J, and additional measurements would be required to separate the respective contributions. We shall discuss this in more detail in Secs. VI A and VII A.

III. EXPERIMENTAL DETAILS

A. Samples

The rare-earth hydroxides from La to Yb and Y are all isostructural, with space group $P6_3/m$. [13] This structure has two molecules per unit cell, but both the rare-earth sites are magnetically equivalent, each having site symmetry C_{3h}. The hydroxides used in our experiments have been grown at Yale by Mroczkowski using a hydrothermal technique which is described elsewhere. [14] This method produces needle-shaped single crystals of which the largest were only 1–10 mg in weight. In order to obtain well-resolved pair lines, the Gd^{3+} concentration had to be limited to about 1%. This necessitated a careful selection of only high-quality crystals to ensure optimum resolution of all the pair transitions. The selected crystals were x-ray oriented so that both a nearest-neighbor and a next-nearest-neighbor bond axis were contained in a horizontal plane. [16] With the sample in the cavity, the magnetic field could then be aligned along either axis by simply rotating the magnet.

The lattice parameters for $Y(OH)_3$, $Eu(OH)_3$, and $Gd(OH)_3$ are listed in Table I together with the nearest- and next-nearest-neighbor pair separations. The dipole constants $g^2\mu_B^2/r_{12}^3$ calculated from these values are also shown. The relatively large error limits reflect uncertainties in the lattice parameters due to apparent variations between different determinations. It is not clear if these arise from small departures of stoichiometry or from poor experimental techniques. In any case the effects are quite small and covered by the quoted error limits.

B. Apparatus

All the measurements reported in this paper were made on a K-band spectrometer operating near 23.0 GHz. The experimental arrangement was generally similar to that which was used previously (see paper I, Ref. 4), except for the actual microwave parts which were changed from a 115-kHz modulated-transmission system to a higher-sensitivity superheterodyne reflection system. The design was conventional, [17] with the carrier signal being used to stabilize the main oscillator to the cavity frequency and a second feedback loop to lock the local oscillator at a fixed frequency difference of 60 MHz from the main klystron frequency. The magnetic field was supplied by a 12-in. Varian Field-Dial magnet and measured with NMR. The field was modulated at 40 to 50 Hz and the signal was phase-sensitively detected at this frequency. A double-Dewar system allowed measurements at 77 and 4.2 K, but most experiments were made only at 77 K.

In view of the extremely limited size of samples available and the generally weak intensity of the pair spectra, it was necessary to check the sensitivity of the system. This was done using a 1-mg sample of MgO doped with 0.034-at.% Cr^{3+} which contained approximately 10^{15} Cr^{52} ions and 10^{14} Cr^{53} ions. [18] The results indicated a limit of detection equivalent to 5×10^{11} $S=\frac{1}{2}$ spins with a 1-Oe linewidth at 77 K and 23.0 GHz. This number can be compared to the expected signal from a typical

TABLE I. Lattice parameters and calculated dipole coupling constants for Gd^{3+} in $Y(OH)_3$, $Eu(OH)_3$, and $Gd(OH)_3$.

$R(OH)_3$	a (Å)[a]	c (Å)[a] ($=r_{nn}$)	Dipolar constant[b] α_{nn} (10^4 cm^{-1})	r_{nnn} (Å)	Dipolar constant[b] α_{nnn} (10^4 cm^{-1})
$Y(OH)_3$	6.25±0.03	3.53±0.03	390±10	4.02±0.03	265±6
$Eu(OH)_3$	6.32±0.03	3.63±0.03	358±9	4.08±0.03	253±6
$Gd(OH)_3$	6.30±0.03	3.61±0.03	365±9	4.06±0.03	256±6

[a]Lattice parameters from Klevtsov and Sheina (Ref. 15). These are in agreement with our own x-ray diffractometer measurements (Ref. 14).

[b]Calculated from $\alpha = g^2\mu_B^2/r^3$, using the g values given in Table II. For $Gd(OH)_3$ we take $g = 1.992$, the same value as that for $Y(OH)_3$.

hydroxide sample. For a 1-mg sample doped with 1-at.% Gd^{3+} there are approximately 6×10^{14} isolated nn pairs which undergo transitions with linewidths of 20–40 Oe. Consequently, the sensitivity required of the spectrometer to detect the most intense pair transitions is equivalent to the detection of only $(2-5)\times10^{13}$, $\delta H = 1$ Oe, $S = \frac{1}{2}$ spins. It is thus evident that the largest nn pair lines should have a signal-to-noise ratio of better than 50 to 1, but some of the less strongly allowed transitions will only be barely detectable. In particular, many of the smaller lines, which in the present case are the most sensitive to the isotropic interactions, are calculated to be very near the limit of the spectrometer resolution, and care had to be used to ensure optimum operation of the system. In practice, about 40 transitions could be observed for each type of pair and this might be expected to be quite adequate for determining the parameters in the corresponding spin Hamiltonian. (See, however, Sec. VI A.)

IV. EXPERIMENTAL RESULTS

A. Single-Ion Spectra

The spectrum of isolated Gd^{3+} ions in $Y(OH)_3$ has previously been observed at 77 K by Scott[19] and we summarize the derived spin-Hamiltonian parameters in Table II. Identical results were obtained for our own Gd^{3+}-doped $Y(OH)_3$ crystals, confirming the fact that our method of mounting the samples (using Apiezon N-grease) did not strain the crystals significantly. Similar results were obtained for the single-ion spectrum of 1-at.% Gd^{3+} in $Eu(OH)_3$ at 77 K. The seven observed transitions were identified from the relative intensities of the lines at nitrogen and helium temperatures and analyzed in the usual manner.[19,20] The corresponding spin-Hamiltonian parameters are shown in Table II. It can be seen that these parameters are very similar in both sign and magnitude to the ones for Gd^{3+} in $Y(OH)_3$.

The small apparent difference between the g values for Gd^{3+} in $Y(OH)_3$ and $Eu(OH)_3$ was checked by a careful comparison of the $|+\frac{1}{2}\rangle \rightarrow |-\frac{1}{2}\rangle$ transition with the resonance in diphenyl picaryl hydrazyl (DPPH). Although the difference was very small, it was just beyond the limit of the combined errors, and in Sec. VII D we shall interpret the shift in terms of an interaction between the Gd^{3+} and Eu^{3+} ions similar to that previously observed in garnets[21] and tricholorides.[5]

B. $Y(OH)_3$:Gd^{3+} Pair Spectra

1. Nearest Neighbors

The EPR spectrum of Gd^{3+} in $Y(OH)_3$ at 77 K and 24.000 GHz, with the magnetic field along the c axis is shown in Fig. 1. In addition to the seven central single-ion lines, many smaller lines may be seen at both high and low fields, extending almost 5000 Oe to either side of the central transition at 8610 Oe. Typical peak-to-peak widths on this derivative trace are about 30 to 50 Oe, corresponding to an experimental resolution of about ±7 Oe. The obvious symmetry of extra lines characterizes them as part of the nearest-neighbor pair spectrum. This is supported by their angular variation, shown in Fig. 2, in which all the lines can be seen to turn symmetrically about the c axis, as ex-

TABLE II. Spin Hamiltonian parameters for single Gd^{3+} ions in $Y(OH)_3$ and $Eu(OH)_3$ at $T = 77$ K.

Parameter	$Y(OH)_3$[a]	$Eu(OH)_3$[b]
g[c]	1.992±0.001	1.990±0.001
b_2^0	−130.4±0.6[d]	−144.9±1.2[d]
b_4^0	−2.2±0.2[d]	−3.0±0.4[d]
b_6^0	+0.60±0.2[d]	+0.6±0.4[d]
b_6^6	±5.3±0.3[d]	±6.0±0.6[d]

[a]After Ref. 19.

[b]This work.

[c]$g = g_\parallel = g_\perp \pm 0.001$.

[d]Units of 10^{-4} cm^{-1}.

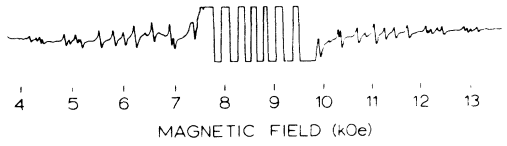

FIG. 1. Nearest-neighbor pair spectrum of Gd^{3+} in $Y(OH)_3$ at $T=77$ K and $\nu=24.000$ GHz, with magnetic field along the c axis.

pected on the basis of the discussion of Sec. II. The field splittings from the central transition for both high- and low-field pair lines are listed in Table III. The final column of Table III measures the average asymmetry of each transition about the center and it can be seen that this is generally even smaller than the expected resolution of ±7 Oe. Moreover, the center of the pair spectrum coincides with that for the single ions, so that the g value of the pairs is identical to the g values of the isolated Gd^{3+} ion.

2. *Next Nearest Neighbors*

When the magnetic field was applied along a nnn bond direction (64° from the c axis), the EPR spectrum shown in Fig. 3 was measured at 77 K and 23.311 GHz. The most pronounced feature of this spectrum was the sharp cutoff for fields greater than 2700 Oe from the central transition. However, the high density of lines and relatively large linewidths (30–50 Oe) made resolution of closely spaced lines quite difficult, particularly around $\Delta H = 2300$ Oe. In addition, the intensities of the pair lines were somewhat smaller than the corresponding nearest-neighbor lines, mainly because

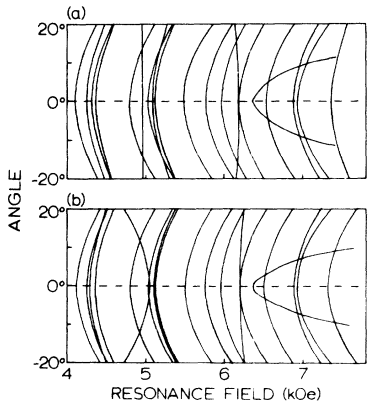

FIG. 2. Angular variation about the c axis of the low-field nn pair lines of Gd^{3+} in $Y(OH)_3$ at $\nu=24.000$ GHz. (a) Experimental spectrum at $T=77$ K; (b) calculated spectrum using the parameters $g=1.992$, $J=0.1264$ cm^{-1}, $\alpha=0.0372$ cm^{-1}, $b_2^0=-0.00378$ cm^{-1}, $b_4^0=-0.00031$ cm^{-1}, $b_6^0=0.00006$ cm^{-1}.

TABLE III. Relative fields (in Oe) of nn pair lines in $Y(OH)_3$ with respect to the central Gd^{3+} single-ion transition ($H_0=8610$ Oe) at 24.000 GHz and 77 K. The last column gives the means shift about H_0.

ΔH_-	ΔH_+	$\frac{1}{2}(\Delta H_+ + \Delta H_-)$
−4519	4521	+1.0
−4362	4361	−0.5
−4318	4320	+1.0
−4252	4245	−3.5
−3819	3824	+2.5
−3703	3701	−1.0
−3583	3591	+4.0
−3518	3514	−2.0
−3490	3501	+5.5
−3119	3116	−1.5
−2843	2838	−2.5
−2635	2631	−2.0
−2429	2425	−2.0
−2214	2217	+1.5
−2075	2072	−1.5
−1730	1728	−1.0
−1674	1669	−2.5
−1269	1265	−2.0

there are only half as many equivalent nnn pairs as there are nn pairs. Taken together, these effects made the empirical determination of the spectrum much harder, and correspondingly increased the difficulty in fitting the spectrum. The quality of this particular spectrum was undoubtedly the poorest of the four discussed in this paper, but as we shall see, it was still adequate for a relatively accurate determination of the spin-Hamiltonian parameters.

The angular variation of the low-field half of the spectrum, which is shown in Fig. 4, revealed an added complication. The pair lines did not quite turn symmetrically about the nnn bond axis, the turning angle varying from line to line by as much as 10° from this axis. Similar behavior was observed by Birgeneau *et al.*[5] for the nnn Gd^{3+} pairs in $EuCl_3$, and it was ascribed to neglected off-diagonal crystal field terms. Since the single-ion crystal field parameters for Gd^{3+} in $Y(OH)_3$ are in fact larger than the corresponding terms in $EuCl_3$, a similar explanation for the asymmetric turning values for the nnn pair lines in $Y(OH)_3$ is not unreasonable in the present case. Table IV lists the high- and low-field splittings from the central transition at $H_0=8360$ Oe, together with the average shift about this point. In spite of the difficulties mentioned above, most of the measured lines were found to correspond to a mean shift relative to H_0 which is less than the experimental resolution of ±7 Oe. As a result of the scatter it was not possible to determine the corresponding g value for nnn pairs very accurately, but it is clearly very

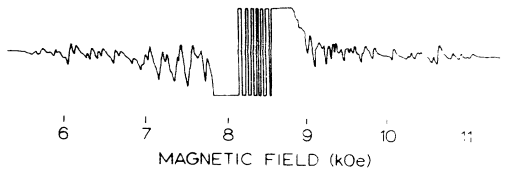

FIG. 3. Next-nearest-neighbor pair spectrum of Gd^{3+} in $Y(OH)_3$ at $T=77$ K and $\nu=23.311$ GHz, with the magnetic field along the calculated nnn bond axis.

close to that for the single ions and nn pairs, as we would expect.

C. $Eu(OH)_3:Gd^{3+}$ Pair Spectra

1. Nearest Neighbors

Figure 5 illustrates the Gd^{3+} pair spectrum in $Eu(OH)_3$ at 77 K and 23.376 GHz for the magnetic field applied along the c axis of the crystal. The spectrum extends to well beyond 5000 Oe to either side of the central single-ion transition at $H_0=8394$ Oe. The outer lines exhibit an obvious symmetry about this field, characteristic of nearest-neighbor pair lines. These pair lines are somewhat narrower than those for the nn pairs in $Y(OH)_3$, with linewidths of about 20 to 30 Oe. The angular variation of the low-field half of the spectrum is shown in Fig. 6 and it can be seen to correspond to the expected symmetric turning of these lines about the c axis. Table V gives the field splittings of corresponding pair transitions at high and low fields and the mean shifts relative to H_0. Because these shifts are predominantly of one sign, the average difference between the center of the single-ion

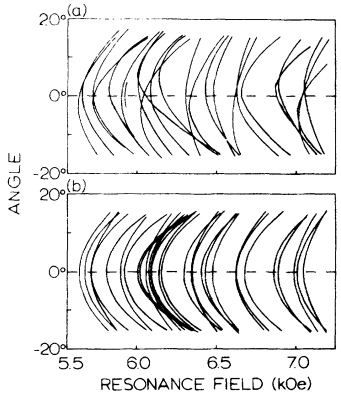

FIG. 4. Angular variation about the calculated nnn bond axis of low-field nnn pair lines of Gd^{3+} in $Y(OH)_3$ at 23.311 GHz. (a) Experimental spectrum at $T=77$ K; (b) calculated spectrum using the parameters $g=1,992$, $J=-0.0059$ cm^{-1}, $a=0.02605$ cm^{-1}, $b_2^0=0.00480$ cm^{-1}, $b_4^0=-0.00010$ cm^{-1}, $b_6^0=0.00003$ cm^{-1}.

TABLE IV. Relative fields (in Oe) of nnn pair lines in $Y(OH)_3$ with respect to the central Gd^{3+} single-ion transition ($H_0=8360$ Oe) at 23.311 GHz and 77 K. The last column gives a measure of the asymmetry of the spectrum.

ΔH_-	ΔH_+	$\frac{1}{2}(\Delta H_- + \Delta H_+)$
−2699	2706	+3.5
−2631	2657	+13.0
−2540	2570	+15.0
−2460	2465	+2.5
−2471	2465	+19.0
−2312	2285	−13.5
−2284	2285	+0.5
−2209	2227	+9.0
−2065	2068	+1.5
−2018	2012	−3.0
−1932	1944	+6.0
−1881	1904	+11.5
−1731	1729	−1.0
−1667	1690	+11.5
−1516	1482	−17.0
−1478	1482	+2.0
−1372	1359	+6.5
−1317	1342	+12.5

spectrum and the center of the pair spectrum is not zero in the present case, and taking the mean we find a shift of −2.1 Oe. That is to say, the nn pair spectrum exhibits a g shift of

$$\Delta g(\text{nn}) = g(\text{nn pairs}) - g(\text{ion}) = +0.0006$$

with respect to the single-ion central field. We shall consider this further in Sec. VII D.

It is also evident from Fig. 5 that there are many additional lines quite close to H_0 which are not listed in Table V. These transitions generally originate from more distant pairs of ions, although there also are some lines due to nearest neighbors among them. In fact, when fitting the spectrum, one test of any calculated set of lines will be to look for a match with some of the previously unidentified lines.

Finally, it is interesting to compare the nn spectra in $Y(OH)_3$ and $Eu(OH)_3$, which we might perhaps have expected to be quite similar, given the small differences in the lattices and the almost identical

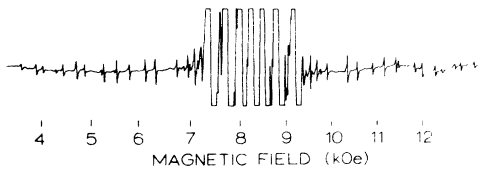

FIG. 5. Nearest-neighbor pair spectrum of Gd^{3+} in $Eu(OH)_3$ at $T=77$ K and $\nu=23.376$ GHz, with the magnetic field along the c axis.

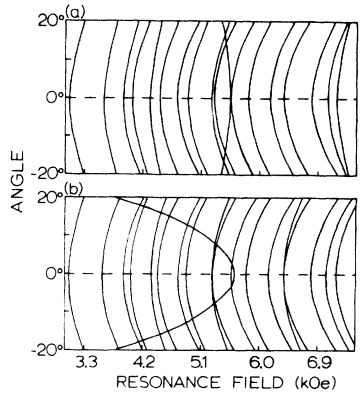

FIG. 6. Angular variation about the c axis of the high-field nn pair lines of Gd^{3+} in $Eu(OH)_3$ at 23.376 GHz. (a) Experimental spectrum at $T=77$ K; (b) calculated spectrum using the parameters $g=1.990$, $J=0.1258$ cm^{-1}, $\alpha=0.03562$ cm^{-1}, $b_2^0=-0.01855$ cm^{-1}, $b_4^0=-0.00037$ cm^{-1}, $b_6^0=0.00005$ cm^{-1}.

single-ion spectra. However, from Figs. 1 and 5 we see that the two spectra do not in fact show any obvious correspondence, illustrating the necessity of a detailed fit using the complete spin Hamiltonian for making any meaningful comparison.

2. *Next Nearest Neighbors*

The last spectrum to be analyzed is the nnn pair spectrum for Gd^{3+} in $Eu(OH)_3$. This is shown in

TABLE V. Relative fields (in Oe) of the nn pair lines in $Eu(OH)_3$ with respect to the central Gd^{3+} single-ion transition ($H_0=8394$ Oe) at 23.376 GHz and 77 K. The last column gives a measure of the asymmetry of the spectrum. The mean shift corresponds to a g-value shift Δg(nn pairs) $=+0.0006$.

ΔH_-	ΔH_+	$\frac{1}{2}(\Delta H_+ + \Delta H_-)$
−5336	5336	0
−4799	4790	−4.5
−4501	4492	−4.5
−4358	4360	+1.0
−4084	4076	−4.0
−3946	3941	−2.5
−3673	3666	−3.5
−3506	3500	−3.0
−3144	3146	+1.0
−3100	3100	0
−2850	2846	−2.0
−2768	2766	−1.0
−2584	2578	−3.0
−2244	2237	−3.5
−2034	2029	−2.5
−1594	1586	−4.0
−1354	1357	+1.5
−1218	1210	−4.0
	Mean shift	−2.1

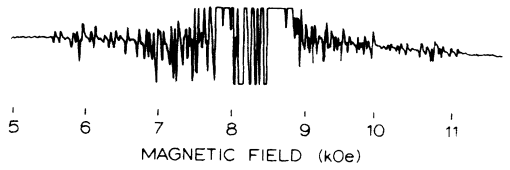

FIG. 7. Next-nearest-neighbor pair spectrum of Gd^{3+} in $Eu(OH)_3$ at $T=77$ K and $\nu=23.372$ GHz, with the magnetic field along the calculated nnn bond axis.

Fig. 7 for the magnetic field at 64° to the c axis, which is the calculated next-nearest-neighbor bond axis. This spectrum exhibits many similarities to the nnn pair spectrum in $Y(OH)_3$ shown in Fig. 4, particularly the sharp cutoff close to $\Delta H=2700$ Oe, and the high density of lines. Another common feature is the nearly (but not quite) symmetrical angular variation of these lines about the geometrical bond axis, as shown in Fig. 8. Unlike the $Y(OH)_3$ case, however, the narrower lines in $Eu(OH)_3$ permitted resolution of many more of the nearly degenerate lines and a more detailed analysis should be possible. Table VI gives the high- and low-field line splittings from the central transition. No attempt has again been made to determine a g shift relative to either the single-ion or nn pair values, since any such effect would be masked by the small irregularities in the turning points of the individual lines. It should be noted, however, that most of the mean shifts from the spectrum center do in fact fall within the experimental resolution of ±7 Oe, although there are several exceptions. In any case, it would seem clear that the g value of the nnn pairs in $Eu(OH)_3$ will be quite close to that of the single ions and nn pairs and that any second-order shifts such as

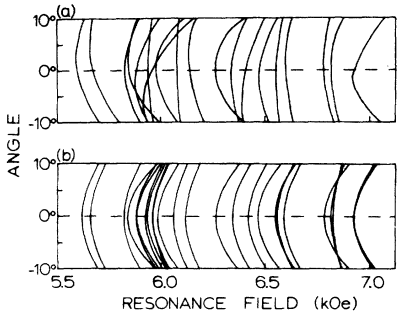

FIG. 8. Angular variation about the calculated nnn bond axis of the low-field nnn pair lines of Gd^{3+} in $Eu(OH)_3$ at $\nu=23.372$ GHz. (a) Experimental spectrum at $T=77$ K; (b) calculated spectrum using the parameters $g=1.990$, $J=-0.01460$ cm^{-1}, $\alpha=0.02531$ cm^{-1}, $b_2^0=0.00201$ cm^{-1}, $b_4^0=0.00002$ cm^{-1}, $b_6^0=-0.00003$ cm^{-1}.

TABLE VI. Relative fields (in Oe) of the nnn pair lines in $Eu(OH)_3$ with respect to the central Gd^{3+} single-ion transition ($H_0 = 8391$ Oe) at 23.372 GHz and 77 K. The last column gives a measure of the asymmetry of the spectrum. The relatively large scatter is probably due to second-order crystal field effects and the mean shift of -4.5 Oe is not really significant.

ΔH_-	ΔH_+	$\frac{1}{2}(\Delta H_+ + \Delta H_-)$
−2795	2779	−8.0
−2722	2677	−22.5
−2567	2575	+4.0
−2546	2528	−9.0
−2510	2482	−14.0
−2453	2457	+2.0
−2433	2414	−9.5
−2413	2414	+0.5
−2315	2338	+11.5
−2256	2261	+2.5
−2124	2126	+1.0
−2049	2055	+3.0
−1983	1969	−7.0
−1916	1924	+4.0
−1827	1830	+1.5
−1827	1789	−19.0
−1612	1587	−12.5
−1569	1587	+9.0
	Mean shift	−4.5

we might expect from the Gd^{3+}-Eu^{3+} interaction must be very small.

V. IDENTIFICATION AND FITTING OF THE EXPERIMENTAL SPECTRUM

A. Spectral Identification

If we assume that the pair Hamiltonian of Eq. (2) provides an adequate description of the spin interactions between Gd^{3+} ions, we are still left with the sizable problem of fitting the experimental spectrum and extracting values of the pair parameters. This problem divides into two parts. First, each line of the experimental spectrum must be identified as belonging to a particular theoretical transition. This is equivalent to estimating an initial set of parameters. Second, the best set of parameters must then be obtained by adjusting the parameters in a least-squares fit of the theoretical spectrum to the experimental line positions, under the constraint that the line identifications remain fixed. Under this procedure every initial identification of the spectrum produces a set of interaction constants, and the final set of parameters is determined from the particular identification which corresponds to the minimum rms deviation between experimental and calculated line positions. In practice, there is usually no ambiguity since one identification generally fits the spectrum noticeably better than any other.

Hutchings *et al.* (Papers I and II) have discussed various aspects of this procedure of identifying and fitting the spectra in their analysis of the Gd^{3+} pairs in the trichlorides. One of the most significant was that the dipolar contribution α could be estimated quite accurately from the formula, $g^2\mu_B^2/r_{12}^3$, and we will show this is also true for the hydroxides. Hence, the initial stage of the problem has been reduced to estimating the isotropic exchange J and the leading crystal field component b_2^0. In the remainder of this section we give a general description of the fitting problem which is intended to supplement the remarks made in the earlier papers.

The Gd^{3+} pair spectra arising from the Hamiltonian of Eq. (1) has been solved numerically in I for $|J| \leq 33\alpha$ and $V_c \equiv 0$. We reproduce this result in Fig. 9, which shows the pair resonance field splittings ΔH as a function of the exchange J, both normalized by the dipole constant α. Inspection of this figure indicates that the theoretical spectra can be divided according to values of J/α into two regions, given approximately by $|J/\alpha| \geq 1.5$ and $|J/\alpha| \leq 1.5$. These two regions present quite different problems in the actual identification of the lines arising from quite different characteristics of the resonance spectra.

In the first region (I), $|J| \geq 1.5\alpha$, the transitions are reasonably well separated from each other, and the total spectrum extends over a wide field range. Moreover, the line intensities generally decrease with increased splitting from the central field H_0, with the result that a corresponding experimental spectrum should be observed to vanish gradually into the noise on either side of H_0. This region has another important feature which is also evident from Fig. 9: The spectra, except for a few of the less intense lines, are insensitive to the exact value of J, particularly when the exchange is antiferromagnetic. J must then be determined by fitting the weaker transitions. Consequently, when b_2^0 is negligible, the line identifications can be made straightforwardly from Fig. 9. When b_2^0 cannot be neglected, the problem is considerably more complex, but b_2^0 is then the only unknown parameter affecting all the line positions. In this case, the identifications can be assigned from a plot of the resonant field splittings as a function of b_2^0 for a constant J and α. Figure 10 shows such a plot for $J/\alpha = 3$ and $\alpha = 0.0368$ cm^{-1}. Evidently, crystal field parameters of the order of the single-ion value [$b_2^0 = -0.013$ cm^{-1} for $Y(OH)_3$: Gd^{3+}] have a significant quantitative and qualitative effect on the pair spectrum. Comparisons of the observed spectrum with figures such as Fig. 10 generally lead to reasonable starting values for the parameters, although several attempts may be necessary to sort out lines which are nearly degenerate. However, once the appropriate range has been identified, the

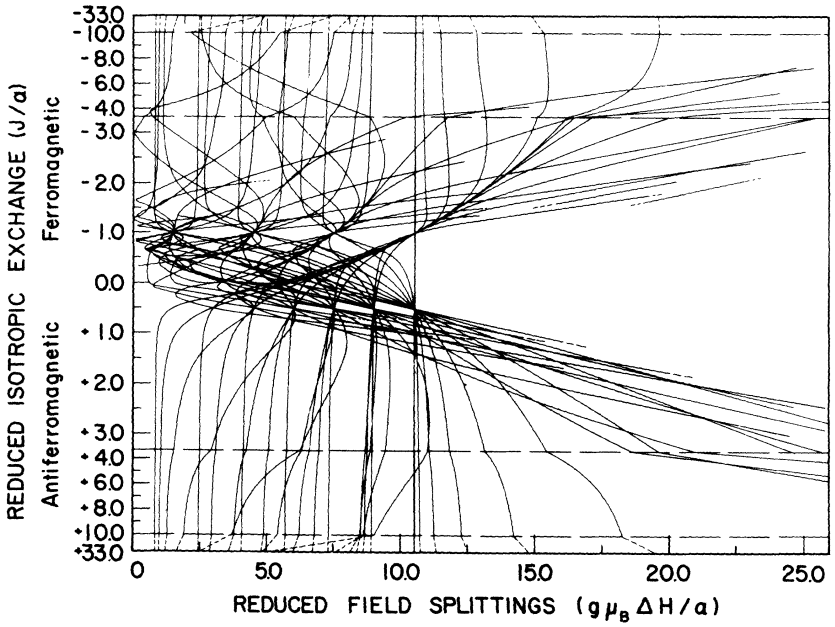

FIG. 9. Theoretical spectra for pairs described by Eq. (2) with $b_2^0 = b_4^0 = b_6^0 = 0$. The reduced field splittings $g\mu_B \Delta H/\alpha$ are shown as a function of the reduced exchange interaction J/α. The lines plotted are those with intensities above about $\frac{1}{50}$ of that of the strongest of the pair lines (after Ref. 4).

convergence of the procedure can be quite rapid.

For the second region (II), $|J| \leq 1.5$, the characteristics of the spectra are very different. Reference to Fig. 9 indicates a very high density of lines with field splittings which extend out to a definite cutoff value. In addition, the line intensities do not exhibit any monotonic behavior, but are more or less random. Even for $b_2^0 \equiv 0$ the high line density complicates the identification of the experimental transitions, and when the crystal field is not small, the theoretical spectrum is further scrambled in a manner analogous to that shown in Fig. 10. In this case one must replot the line positions as a function of b_2^0 for many closely spaced values of J. That is to say, the fitting procedure in this regime is a function of two unknown parameters, J and b_2^0, and is generally much more complicated than in the first regime. Consequently, it may be necessary to consider additional information such as the temperature dependence of the line intensities, special groupings of the spectra which occur around $J/\alpha = 0.5$ and -1.0 (see Fig. 9), or estimates of the J and b_2^0 values determined in other experiments.

B. Fitting Procedure

Once a preliminary identification of the spectrum had been made, the best parameters for that identification were determined by a least-squares routine using a program written by Powell.[22] The individual transitions could then be relabeled and another set of parameters generated until a fit to the entire spectrum was obtained. (This was the same procedure used in I and II by Hutchings *et al.*)

One aspect of the previous papers which has been improved in the present analysis is a more systematic estimation of the errors to be assigned to the various fitted parameters. The approach we have taken is to estimate the standard deviations of the parameters directly from the matrix of the least-squares equations.[23] The computer program minimizes the sum of squares of the deviations of the theoretical and experimental resonance fields for M different lines,

$$F = \sum_{n=1}^{M} [H_n(\text{expt.}) - H_n(\text{theor.})]^2 ,$$

and hence the covariance matrix of F with respect to the parameters i and j, B_{ij}, is the inverse of the matrix of the least-squares equations. If N parameters are fitted to obtain $F_{\min}$, the best estimate of the standard deviation of the ith parameter is thus

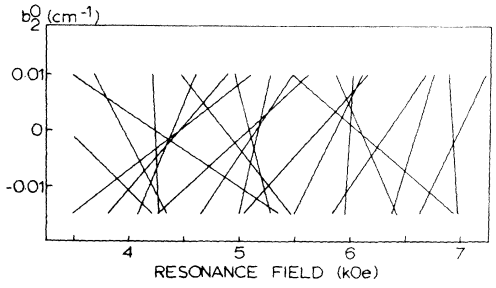

FIG. 10. Vairation of the calculated low-field pair spectrum as a function of b_2^0 at $\nu = 24.000$ GHz, with $g = 1.992$, $J = 0.1134$ cm^{-1}, $\alpha = 0.0368$ cm^{-1}, and $b_4^0 = b_6^0 = 0$.

$$\sigma_i = [B_{ii} \cdot F_{\min}/(M-N)]^{1/2} .$$

This takes into account the correlation between the various parameters for a case such as ours in which the parameters do not contribute to F independently. It is this number, σ_i, which we quote throughout as the uncertainty of the ith fitted parameter.

It is important to note that these standard deviations are defined relative to the Hamiltonian of the system. The omission of any important terms from the Hamiltonian represents a systematic error which the σ_i cannot include. Furthermore, the σ_i are dependent on the particular identification of the spectrum, so that an improper label for any transition is another systematic discrepancy for which the σ_i cannot account. Generally, the correct identification can be found by trail and error as long as the form of the Hamiltonian remains fixed. If additional terms are added to the fitting equations it is necessary to recheck the line identifications, since a better fit might be possible with a somewhat different labeling of the nearly degenerate transitions.

VI. ANALYSIS OF THE PAIR SPECTRA

In Sec. V, the general procedure for identifying and fitting the various pair spectra was described in some detail. Although the relative size of the parameters was indicated by the main characteristics of the experimental spectra, it proved to be useful to have some independent information about the strength of the various interactions. Such an estimate was available to us from the high-temperature ($T \gg T_N$) susceptibility and specific-heat measurements on concentrated $Gd(OH)_3$ by Skjeltorp *et al.*,[6] who derived $J_{nn} = 0.125 \pm 0.004$ cm^{-1} and $J_{nnn} = -0.012 \pm 0.007$ cm^{-1}, while approximate values for the dipolar terms could be readily calculated from the lattice parameters, as listed in Table I. For both $Y(OH)_3$ and $Eu(OH)_3$ the nearest-neighbor pairs should thus be characteristic of region I with $J_{nn}/\alpha_{nn} \sim 3$, but the next-nearest-neighbor pairs should show a spectrum characteristic of region II with $J_{nnn}/\alpha_{nnn} \sim -0.3$. From the description of the experimental spectra in Sec. IV, it was apparent that this general classification was valid. Finally, the leading crystal field parameter b_2^0 was estimated to be of the same order of magnitude as the value for the single-ion spectrum, although the pair value would be expected to be somewhat different, owing to the distortion of the lattice around a pair.

Because of the similarities in the spectra of a given type of neighbor, we shall proceed to discuss the nearest-neighbor pair results for both $Y(OH)_3$ and $Eu(OH)_3$ hosts before analyzing the next-nearest-neighbor data.

A. Nearest-Neighbor Pairs

1. $Y(OH_3)$: Gd

Using the parameters listed above, the pair spectrum was calculated and compared with the nn spectrum for Gd^{3+} in $Y(OH)_3$. No match between these spectra could be made. From the general features of the spectrum and the above parameter estimates, it seemed fairly certain that the interactions must be close to the estimates value $J_{nn}/\alpha_{nn} \sim 3$, and thus only a better estimate of b_2^0 could resolve the problem. To find b_2^0 appropriate to the nn pairs, calculated spectra were plotted as a function of b_2^0 for $J/\alpha = 3$, as shown in Fig. 10. Even though the individual resonances vary quite linearly with b_2^0, the over-all result for even small changes in b_2^0 was to change significantly the general appearance of the spectrum. By superimposing the experimental spectrum on this plot, a close correspondence was found near $b_2^0 = -0.005$ cm^{-1}, particularly for the more intense lines between 5.5 and 7.5 kOe. With an initial set of line identifications made from these parameters, several least-squares-fitting runs were necessary to sort out the best fit to all the line positions. The parameters corresponding to the best fit (with $\mathcal{H}_{int}^{(1)}$ set $\equiv 0$) and a comparison between calculated and observed individual line positions are given in column A of Table VII. Figure 11 shows a comparison of both the observed and calculated line positions and their relative intensities. It can be seen that the over-all correspondence of the two spectra is quite good, confirming the correct identification of individual lines with corresponding transitions.

The parameters obtained in this fit are generally consistent with values from other sources. In particular, the isotropic exchange is *antiferromagnetic* in sign and very nearly equal to the value obtained for $Gd(OH)_3$,[6] as might be expected from the close match in lattice parameters and the general trend of the exchange with ion separation.[7] The dipolar coupling constant is intermediate between the values calculated for $Gd(OH)_3$ and $Y(OH)_3$, but somewhat closer to the former than might be expected. The second-order crystal field parameter b_2^0 has shifted considerably from the single-ion value, although the fourth- and sixth-order terms (b_4^0 and b_6^0) are identical, within the error limits, to the single-ion values.

The root-mean-square deviation of the calculated line positions from the measured values was 27 Oe, compared with linewidths of more than 40 Oe, and splittings up to 4500 Oe from H_0. Nevertheless, this deviation was well beyond the resolution of the line positions and their symmetry about H_0. Examination of Table VII indicated, for example, that the line with $\Delta H = 3702$ Oe and labeled 2, 15 (marked by arrows in Fig. 11) had only been fitted

TABLE VII. Mean experimental and calculated line splittings for nn pair spectrum of Gd^{3+} in $Y(OH)_3$ at 77 K and 23.311 GHz.

		Calculated					
		A: $\mathcal{H}_{int}^{(1)}=0$		B: $\mathcal{H}_{int}^{(1)}=\mathcal{H}(Q)$		C: $\mathcal{H}_{int}^{(1)}=\mathcal{H}(Q^{\|m\|})$	
Label	Experiment ΔH (Oe)	Position	Deviation	Position	Deviation	Position	Deviation
2, 4	1267.5	1286.2	19.2	1264.9	−2.1	1269.5	2.5
2, 8	1671.5	1695.9	24.4	1662.0	−9.5	1665.3	−6.2
3, 1	1729.0	1710.4	−18.6	1699.6	−29.4	1731.2	2.2
3, 4	2073.5	2097.6	24.1	2075.0	1.5	2077.8	4.3
1, 17	2215.5	2207.2	−8.3	2226.2	10.7	2216.3	0.8
4, 1	2427.0	2396.1	−30.9	2389.5	−37.5	2424.1	−2.9
2, 11	2427.0	2438.4	11.4	2420.5	−6.5	2427.7	0.7
3, 7	2633.0	2664.4	31.4	2638.7	5.7	2634.4	1.4
4, 3	2840.5	2864.8	24.3	2849.8	9.3	2846.5	6.0
5, 1	3117.5	3147.0	29.5	3091.4	−26.1	3120.0	2.5
4, 6	3495.5	3514.9	19.4	3500.7	5.2	3488.4	−7.1
3, 10	3516.0	3513.7	−2.3	3515.2	−0.8	3515.1	−0.9
5, 3	3587.0	3601.2	14.2	3596.2	9.2	3585.1	−1.9
2, 15	3702.0	3628.9	−73.1	3677.6	−24.4	3701.6	−0.4
6, 1	3821.5	3788.4	−33.1	3808.4	−13.1	3818.9	−2.6
5, 5	4248.5	4277.1	28.6	4265.5	17.0	4250.7	2.2
6, 2	4319.0	4334.9	15.9	4333.5	14.5	4318.6	−0.4
4, 8	4362.5	4366.7	4.2	4367.9	5.4	4362.7	0.2
7, 1	4520.0	4500.1	−19.9	4545.7	25.7	4521.6	1.6
RMS deviation (Oe)		27		17		3.2	
Fitted parameters (10^{-4} cm^{-1})							
J		1264 ± 55		1880 ± 110		1766 ± 97	
α		372.0 ± 1.3		371.4 ± 0.9		386.6 ± 2.3	
b_2^0		−36.8 ± 3.5		−41.3 ± 4.7		1.0 ± 7.7	
b_4^0		−3.1 ± 0.8		−4.2 ± 0.5		−2.0 ± 0.3	
b_6^0		0.6 ± 0.1		0.5 ± 0.6		0.6 ± 0.1	
Q^0		0		18.8 ± 3.3		2.9 ± 4.5	
$Q^{\|1\|}$		0		−18.8 ± 3.3		−4.1 ± 4.2	
$Q^{\|2\|}$		0		18.8 ± 3.3		7.5 ± 3.8	

to 73 Oe, and this was judged to be a significant discrepancy which had to be resolved. In the calculated spectrum this line was found to be nearly degenerate with line 5, 3, in contrast to the rather large separation indicated experimentally. If we assume that the observed line is spurious and not 2, 15 and ignore it in the fit, the rms deviation improves by a factor of 2 to about 14 Oe without a significant change in any of the pair parameters. This was the situation described in our earlier report.[24]

Subsequently, however, several other samples were examined to test the possibility that the experimental lines at $\Delta H = \pm 3702$ Oe might be due to an impurity, but identical results were in fact obtained for samples from different batches and with different Gd^{3+} concentrations. This fact together with the symmetry about H_0 and the angular turning point around the c axis established that these transitions must almost certainly be part of the nn pair spectrum and thus cannot be ignored. Moreover, the relative intensity of these transitions and the characteristic low-field angular variation (see Fig. 3) suggested that 2, 15 was in fact the correct label, as assigned previously (Table VII). Consequently, we have to conclude that the Hamiltonian $\mathcal{H}^{(0)}$ can only describe the entire spectrum to within 27 Oe, rms, and the particular line 2.15 only to within 73 Oe. Similar discrepancies will be encountered for nn Gd^{3+} pairs in $Eu(OH)_3$ to be described in Sec. VI A 2, in marked contrast to the corresponding deviations for nn pairs in $LaCl_3:Gd$[4] and $EuCl_3:Gd$,[5] which were only 5 and 7 Oe, respectively. We must conclude therefore that there is

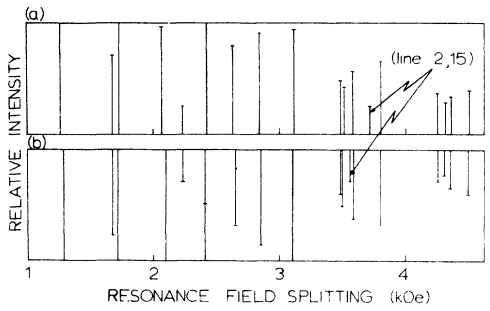

FIG. 11. Best fit to the nn pair line splittings and intensities of Gd^{3+} in $Y(OH)_3$. (a) Experimental spectrum at $T=77$ K; (b) calculated spectrum using the parameters $g=1.992$, $J=0.1264$ cm^{-1}, $\alpha=0.03720$ cm^{-1}, $b_2^0=-0.00368$ cm^{-1}, $b_4^0=-0.00031$ cm^{-1}, $b_6^0=0.00006$ cm^{-1}.

a significant difference between the hydroxides and trichlorides which has not been taken into account in our choice of $\mathcal{H}^{(0)}$.

In considering additional terms which might be added to the Hamiltonian we can use the high degree of symmetry of the observed pair lines about H_0 to eliminate all terms which do not commute with T_z. There are only two possible bilinear terms which satisfy this condition, an anisotropic exchange term of the type $J_a S_{z1} S_{z2}$ and an antisymmetric term of the form $d(S_{x1}S_{y2} - S_{y1}S_{x2})$. The former is already represented in Eq. (1) if we allow α to be replaced by $\alpha' = \alpha - \frac{1}{3}J_a$ and J by $J' = J + \frac{1}{3}J_a$. Inasmuch as both J and α were allowed to vary freely in the fitting procedure, no improvement can be obtained from such a term. The antisymmetric term can also be eliminated, using the inversion symmetry of a nn pair in the hydroxide structure. However, since it is just possible that the formation of a nn pair might destroy this symmetry and thus allow an antisymmetric term, we tried several fitting runs with d allowed to vary, but in fact no improvement of the fit resulted. It thus became apparent that the discrepancies in the nn spectrum of $Y(OH)_3$: Gd could not be accounted for by the addition of further *bilinear* terms to $\mathcal{H}^{(0)}$.

Possible biquadratic terms consistent with the spectral symmetry have already been considered in Sec. II and are summarized in operator-equivalent form in Eq. (3). In our first attempt to include biquadratic terms we considered only the usual isotropic term, given in our notation by

$$Q^m = (-1)^m Q.$$

When this term was included in the fitting routine some improvement resulted, as may be seen from a comparison of columns A and B of Table VII. The rms deviation decreased from 27 to 17 Oe, mostly by reducing the very large discrepancy for line 2, 15. Nevertheless, several calculated lines still show differences of as much as 40 Oe from the experimental resonance fields. We must conclude therefore that isotropic biquadratic exchange can only account for a small part of the discrepancies noted above.

Even though the isotropic biquadratic term in Q had only a small effect on the spectrum and the other parameters, it did produce a striking shift in the fitted value of the isotropic bilinear exchange constant J. This was found for the nn pair fits for both $Y(OH)_3$: Gd and $Eu(OH)_3$: Gd, and it occurred whenever isotropic bilinear and biquadratic terms were fitted together. We shall discuss this effect in detail in Sec. VII A.

As a further refinement, we next tried fitting the data using all three of the independent parameters Q^0, $Q^{|1|}$, and $Q^{|2|}$ of Eq. (3); the results are given in column C of Table VII. It may be seen that the new fit is a dramatic improvement over both previous attempts to describe the experimental spectrum, and, in particular, there are now no large discrepancies for any of the individual lines. The over-all rms deviation is only 3 Oe, well within the experimental resolution uncertainty and it would appear that we have obtained an empirically satisfactory fit.

As in the case of the fit with only Q, there is again a large shift in J relative to the initial fit, but this is now to be expected since we can always decompose the $Q^{|m|}$ into isotropic and anisotropic parts, as in Eqs. (5) and (6). The shift is then associated with the isotropic component, as before, and this will be discussed further in Section VII A.

There are also shifts in some of the other parameters, with α moving towards the value calculated for undoped $Y(OH)_3$ (Table I), as we would expect for a more nearly exact fit. The shifts in the crystal field parameters have no obvious significance, but it is interesting to note that only b_2^0 changes appreciably, while b_4^0 and b_6^0 remained small and essentially unchanged.

2. $Eu(OH)_3$: Gd

In view of the very small dimensional differences between $Y(OH)_3$ and $Eu(OH)_3$, the nn pair spectrum in $Eu(OH)_3$ might be expected to be very similar to that found in $Y(OH)_3$. However, comparison of the observed spectra (Figs. 1 and 5) indicated significant differences, particularly in the grouping of the outer lines, and a total spread of lines some 1500 Oe greater in $Eu(OH)_3$ than in $Y(OH)_3$. Nevertheless, the procedure adopted for $Y(OH)_3$ proved to be equally applicable to the initial identification of these pair lines in $Eu(OH)_3$ and the previous results served as a useful starting point, especially for J and α. A plot of field splittings as a function of b_2^0 for fixed J and α, similar to that in Fig. 10,

TABLE VIII. Predicted line positions (in Oe) for three different Hamiltonians.

Label	$\mathcal{H}^{(1)}_{int}=0$	$\mathcal{H}^{(1)}_{int}(Q)$	$\mathcal{H}^{(1)}_{int}(Q^{|m|})$	Expt.
3, 13	$\Delta H=3880$	3875	3962	3972
2, 18	$\Delta H=3841$	3831	4073	4080
1, 25	$\Delta H=4085$	4003	4619	4598

yielded a close correspondence between the experimental and theoretical spectra for $b_2^0 \sim -0.020$ cm^{-1}, and this allowed a complete identification of the spectral lines. Again, care was necessary to identify the line 2, 15 which had also presented a problem in the $Y(OH)_3$ case. After several fitting runs using only $\mathcal{H}^{(0)}$, the best fit gave an rms deviation of 25 Oe, similar to that found for the nn pairs in $Y(OH)_3$. This fit is shown in Fig. 12. Subsequent attempts to fit the spectrum using first an isotropic biquadratic term Q and then an axial biquadratic interaction reduced the rms deviation to 12 and 3.1 Oe, respectively.

The inclusion of biquadratic terms into the spin Hamiltonian has obviously improved the description of the experimental spectra, but it could be argued that part of this improvement might be due to the fact that the number of parameters used to fit the spectra had increased from five to eight. If the biquadratic terms were really significant they should allow us to *predict* the location of additional transitions with greater accuracy than the truncated Hamiltonian $\mathcal{H}^{(0)}$. Examination of the calculated nn $Eu(OH)_3$ spectra revealed the presence of three more lines, designated at 3, 13, 2, 18, and 1, 25, with intensities only a little less than that of the weakest transition observed up to that point. The predicted line positions were noticeably different for the three different Hamiltonians which we have considered, as the values shown in Table VIII indicate.

Two separate experiments were performed to search for these extra transitions, In the first, the nn pair spectrum of $Eu(OH)_3$ was measured very carefully in the indicated field regions using a multichannel analyser (Fabritek 1052 LSH) to increase the signal-to-noise ratio. A second approach made use of the needle shape of the crystals to make a composite sample consisting of 17 of the largest available crystals glued together with their c axes parallel. This effectively increased the size of the sample by a factor of at least 10 as long as the magnetic field was directed along the common c axis. Experimentally, it was apparent that the alignment of the individual crystals was quite precise since the linewidths of the pair lines from the composite sample were quite close to the linewidths for a single crystal. All three of the previously unobserved lines were found in both of these experiments, with field splittings as listed above. The line 2, 18 was found to be almost degenerate with a larger previously noted transition (4, 8) when the field was along the c axis, but it emerged off axis on the low-field side because of its unique angular variation.

Comparison of the three observed line positions with the values predicted by the full biquadratic fit shows that the agreement is quite spectacular and it clearly reinforces the earlier indication of its importance.

The experimental spectrum including the three new lines was next refitted in three stages as before, and the results are presented in Table IX. In the first attempt with $\mathcal{H}^{(1)}_{int} \equiv 0$, shown in column A of the table, the glaring differences referred to in the previous paragraph have been considerably reduced, but only at the expense of several other transitions, so that the over-all rms deviation is still 36 Oe. In this fit several of the calculated lines were more than 50 Oe from the experimental values, with one differing by as much as 78 Oe. Furthermore, the dipolar constant in this fit was found to lie just outside the range defined in Table I for $Eu(OH)_3$ and $Gd(OH)_3$, a significant discrepancy, since for every other case α has always been found to be between the values calculated for the pure crystals. As was expected, the isotropic biquadratic interaction improved the fit somewhat, reducing the rms deviation from 36 to 29 Oe, but it could not remove the discrepancy in the anisotropic term and hence produced the same value of α as before. The full biquadratic interaction (column C of Table IX) not only reduced the rms deviation to 4.2 Oe, but it also resolved this discrepancy in α.

We can conclude from all this that the anisotropic biquadratic terms are indeed necessary for a proper fit to the spectrum in the present case. A simi-

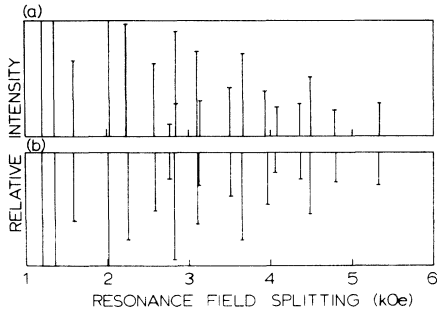

FIG. 12. Best fit to the nn pair line splittings intensities of Gd^{3+} in $Eu(OH)_3$. (a) Experimental spectrum at $T=77$ K; (b) calculated spectrum using the parameters $g=1.990$, $J=0.1258$ cm^{-1}, $\alpha=0.03562$ cm^{-1}, $b_2^0=-0.01855$ cm^{-1}, $b_4^0=-0.00037$ cm^{-1}, $b_6^0=0.00005$ cm^{-1}.

TABLE IX. Mean experimental and calculated line splittings for nn pair spectrum of Gd^{3+} in $Eu(OH)_3$ at 77 K and 23.376 GHz.

		Calculated					
	Experiment	A: $\mathcal{H}_{int}^{(1)} \equiv 0$		B: $\mathcal{H}_{int}^{(1)} = \mathcal{H}(Q)$		C: $\mathcal{H}_{int}^{(1)} = \mathcal{H}(Q^{|m|})$	
Label	ΔH (Oe)	Position	Deviation	Position	Deviation	Position	Deviation
1, 1	414.0	398.3	−15.7	396.1	−17.9	405.6	−8.4
1, 5	456.0	452.5	3.5	454.2	−1.8	455.9	0.1
2, 1	1214.0	1194.4	−19.6	1289.0	−25.0	1215.9	1.9
2, 4	1355.5	1368.5	+13.0	1355.3	−0.2	1359.3	3.8
2, 8	1590.0	1614.9	24.9	1579.4	−10.6	1583.7	−6.3
2, 11	2032.0	2056.0	24.0	1991.3	−40.7	2024.3	−7.7
3, 1	2032.0	1994.5	−37.5	1990.0	−42.0	2029.1	−2.9
3, 4	2242.0	2257.2	15.3	2242.4	0.4	2244.9	2.9
3, 7	2581.0	2618.3	37.3	2583.9	2.9	2579.0	−2.0
1, 21	2767.0	2689.2	−77.8	2739.9	−27.1	2766.2	−0.8
4, 1	2848.0	2800.7	−47.3	2802.4	−45.5	2850.2	2.2
2, 15	2848.0	2866.9	18.9	2845.1	−2.9	2856.0	8.0
4, 3	3100.0	3116.3	16.3	3106.1	6.1	3103.2	3.2
3, 10	3145.0	3183.5	38.5	3150.1	5.1	3142.3	−2.7
4, 6	3503.0	3543.5	40.5	3521.3	18.3	3503.3	0.3
5, 1	3609.5	3618.8	−50.7	3632.4	−37.1	3669.2	−0.3
5, 3	3943.4	3956.1	12.6	3954.4	10.9	3945.0	1.5
3, 13	3940.5	4017.5	45.0	4028.1	55.6	3966.0	−6.5
4, 8	4080.0	4131.7	51.7	4119.9	39.9	4077.1	−2.9
2, 18	4080.0	4095.3	15.3	4124.3	44.3	4072.8	−7.2
5, 5	4359.0	4395.0	36.0	4379.5	20.5	4358.5	−0.5
6, 1	4496.5	4451.9	−44.6	4482.9	−13.6	4499.7	3.2
1, 25	4598.0	4542.9	−55.1	4532.1	−65.9	4595.9	−2.1
6, 2	4795.5	4793.8	−1.7	4800.5	5.0	4790.8	−4.7
7, 1	5336.0	5301.6	−34.4	5355.6	19.6	5335.0	−1.0
RMS deviation (Oe)		36		29		4.2	
Fitted parameters (10^{-4} cm^{-1})							
J		1258 ± 71		3497 ± 713		1720 ± 90	
α		356.2 ± 0.9		355.1 ± 0.8		363.7 ± 0.3	
b_2^0		−185.5 ± 2.1		−192.5 ± 2.3		−168.3 ± 1.4	
b_4^0		−3.7 ± 0.9		−4.7 ± 0.8		−2.4 ± 0.2	
b_6^0		0.5 ± 1.3		0.5 ± 1.0		0.7 ± 0.2	
Q^0		0		+56.8 ± 18.0		7.4 ± 2.3	
$Q^{|1|}$		0		−56.8 ± 18.0		−8.3 ± 2.2	
$Q^{|2|}$		0		+56.8 ± 18.0		11.0 ± 2.2	

lar search for extra lines in the nn spectrum of $Y(OH)_3$:Gd was not attempted since the available crystals were not as good and the linewidths somewhat larger. The chance of finding the rather weak lines was therefore small and it was felt that there was, in any case, enough evidence to support the finding of anisotropic biquadratic interactions also in that system.

Of more immediate interest are the values of the much larger bilinear exchange constants J and the disquieting large variation in the fitted values when the biquadratic term was added. We shall return to this point in Sec. VII A, but we may note already here that some additional experimental information is needed to determine J more precisely. In principle this could be done by finding additional transitions which depend more sensitively on J, but a search for several possible lines failed to show any additional resonances, even though the calculated intensities indicated that they should have been observable. The reason for this is not clear at this time, but it most probably results from some additional line broadening due, perhaps, to the more critical dependence of the resonance on ex-

change—the very effect which we are trying to observe. However, we can also obtain an estimate of the relative importance of J and Q from magnetic susceptibility and specific-heat measurements, and we shall use these results in Sec. VII A to obtain a final set of interaction parameters for the nearest neighbors.

B. Next Nearest Neighbors

1. $Y(OH)_3$: Gd

Bulk properties of $Gd(OH)_3$[6] indicated that the nnn Gd^{3+} pair interactions should be characteristic of region II, $|J| < 1.5\alpha$. The sharp cutoff of the experimental spectrum beyond $|\Delta H| \sim 2700$ Oe lent added support to this estimate. Furthermore, b_2^0 quantized along the nnn bond axis was expected to be small and positive. In spite of this preliminary information, the identification of the spectrum proved to be quite difficult. Several of the more intense lines were almost degenerate, with the exact number of lines being unknown—particularly those lines near $|\Delta H| \sim 2400$ Oe. After plotting several trial spectra calculated from parameters in the vicinity of the above estimates, it became obvious that b_2^0 must be restricted to a limited range in order to satisfy the field cutoff criterion. Subsequently, a tentative identification was made near $J = -0.005$ cm^{-1}, and after a few fitting runs the best fit given in Table X was obtained.

TABLE X. Mean experimental and calculated line splittings for nnn pair spectrum of Gd^{3+} in $Y(OH)_3$ at 77 K and 23.311 GHz. $g = 1.992$; $J = -0.005964$ cm^{-1}; $\alpha = 0.026055$ cm^{-1}; $b_2^0 = 0.004855$ cm^{-1}; $b_4^0 = -0.000086$ cm^{-1}; $b_6^0 = -0.000023$ cm^{-1}.

Label	Experimental	Calculated	Difference
2, 8	1330.0	1316.9	−13.1
1, 9	1365.0	1371.2	+6.2
1, 17	1365.0	1353.7	−11.3
1, 20	1480.0	1473.4	−6.6
2, 17	1499.0	1502.9	3.9
1, 8	1678.0	1638.8	−39.2
1, 24	1678.0	1684.1	6.1
1, 13	1730.0	1730.8	0.8
3, 7	1730.0	1735.9	5.9
4, 1	1892.0	1887.9	−4.1
1, 21	1938.0	1956.9	18.9
2, 11	1938.0	1927.4	−10.6
3, 1	2015.0	2014.3	−0.7
5, 1	2015.0	2021.6	6.6
2, 15	2067.0	2067.1	0.1
2, 1	2218.0	2226.6	8.6
3, 4	2218.0	2219.6	1.6
2, 4	2285.0	2269.5	−15.5
3, 10	2285.0	2273.5	−11.5
4, 3	2285.0	2285.1	0.1
4, 6	2285.0	2285.2	0.2
6, 1	2299.0	2303.2	4.2
1, 1	2313.0	2336.3	23.3
1, 5	2313.0	2340.0	27.0
2, 18	2441.0	2442.3	1.3
5, 3	2463.0	2467.1	4.1
3, 13	2555.0	2555.6	0.6
4, 8	2644.0	2647.3	3.3
7, 1	2644.0	2649.1	5.1
5, 5	2703.0	2689.2	−13.8
6, 2	2720.0	2720.8	0.8

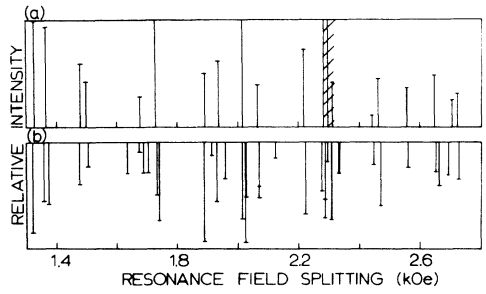

FIG. 13. Best fit to the nnn pair line splittings and intensities of Gd^{3+} in $Y(OH)_3$. (a) Experimental spectrum at $T = 77$ K; (b) calculated spectrum using the parameters $g = 1.992$, $J = -0.00595$ cm^{-1}, $\alpha = 0.02605$ cm^{-1}, $b_2^0 = 0.00480$ cm^{-1}, $b_4^0 = -0.00010$ cm^{-1}, $b_6^0 = 0.00003$ cm^{-1}.

The rms deviation of this fit was 9 Oe, in very reasonable agreement with the expected experimental accuracy and the somewhat anomalous angular variation of some of the lines mentioned previously. No attempt was therefore made to include any higher-order terms into the fit of this spectrum and it seems clear that quite a complicated refinement would be needed in this case to account for both the residual discrepancies and the angular variations. However, all these effects are small[25] and the fit shown in Table X can be considered as quite satisfactory. Figure 13 compares the calculated and experimental line splittings, including the relative intensities of the individual transitions. The agreement here is also quite good, particularly when it is noted that some of the smaller calculated lines are not intense enough to be observed above the experimental noise.

The most remarkable feature of these results is the fact that the next-nearest-neighbor exchange coupling is *ferromagnetic*, but more than an order of magnitude smaller than the nearest-neighbor exchange. This is quite different from the earlier results in the trichlorides, and we shall discuss it further in Sec. VIIB. Both the dipolar and crystal field terms closely approximate the original estimates, as we might expect.

2. $Eu(OH)_3$: Gd

We have already remarked that the general features of the nnn pair spectrum for Gd^{3+} in $Eu(OH)_3$

TABLE XI. Mean experimental and calculated line splittings for the nnn pari spectrum of Gd^{3+} in $Eu(OH)_3$ at 77 K and 23.372 GHz, with $J=-0.01460$ cm^{-1}, $\alpha=0.02527$ cm^{-1}, $b_2^0=0.00200$ cm^{-1}, $b_4^0=0.000025$ cm^{-1}, and $b_6^0=-0.000024$ cm^{-1}.

Label	Experimental	Calculated	Difference
2, 8	1578.0	1565.4	−12.6
3, 7	1578.0	1574.1	−3.9
1, 25	1600.0	1601.8	1.8
1, 13	1808.0	1795.0	−13.0
1, 12	1829.0	1836.4	7.4
1, 8	1829.0	1833.0	+4.0
2, 11	1829.0	1827.9	−1.1
2, 18	1920.0	1919.3	−0.7
4, 6	1976.0	1966.9	−9.1
3, 10	2052.0	2041.4	−10.6
3, 13	2125.0	2119.1	−5.9
5, 1	2259.0	2267.3	8.3
4, 1	2327.0	2324.6	−1.4
4, 8	2413.0	2399.5	−13.5
6, 1	2424.0	2425.0	1.0
3, 1	2455.0	2461.1	6.1
4, 3	2455.0	2461.1	6.1
3, 4	2455.0	2454.1	−0.9
5, 5	2496.0	2496.0	9.1
2, 4	2496.0	2501.3	5.3
2, 1	2496.0	2499.0	3.3
1, 5	2537.0	2457.0	10.0
1, 1	2537.0	2457.0	10.0
5, 3	2571.0	2565.9	−5.1
7, 1	2700.0	2726.3	26.3
6, 2	2786.0	2768.9	−17.1

were both qualitatively and quantitatively similar to those for the nnn pairs in $Y(OH)_3$. The smaller linewidths in the $Eu(OH)_3$ case permitted the resolution of more of the nearly degenerate transitions around $\Delta H=\pm 2400$ Oe. The identification procedure was again quite tedious, however, since many spectra had to be calculated and compared with the experimental line positions and intensities. The sharp cutoff beyond $|\Delta H|\sim 2700$ Oe proved to be a key factor in obtaining a fit, as it had been for the nnn pairs in $Y(OH)_3$. A comparison between the experimental results and the final fit is given in Table XI. The rms deviation for this fit was 9 Oe, the same value as for the $Y(OH)_3$ case. Correspondingly, the experimental and calculated line intensities were again in good agreement, as shown in Fig. 14. As for the nnn pairs in $Y(OH)_3$, no attempt was made to include higher-order terms into the spin Hamiltonian.

The magnitude of the bilinear exchange constant was almost three times larger than the value found for the nnn pairs in $Y(OH)_3$, but it was still only about 10% of the magnitude found for the nn pairs. As in the case of the $Y(OH)_3$ results, the sign was found to be *ferromagnetic*, again in contrast with the antiferromagnetic nn interaction. The fitted dipolar parameter α was found to be very close to the calculated value of 0.0253 cm^{-1} estimated from the $Eu(OH)_3$ lattice constants (see Table I). Also, the crystal field parameters were all found to agree with estimates based on the single-ion values referred to a nnn pair axis.

The over-all fit of the nnn spectra for both the $Y(OH)_3$ and $Eu(OH)_3$ hosts can thus be regarded as quite satisfactory and generally in accord with earlier pair results. The nn results on the other hand are not quite so straightforward, and, in particular, the anomalous biquadratic terms require some further discussion. We shall consider this in Sec. VII.

VII. DISCUSSION

A. Biquadratic Effects

1. Separation of Bilinear and Biquadratic Terms

In the previous sections we noted the fact that the bilinear exchange coefficient J for both the nn spectra was shifted markedly whenever isotropic biquadratic terms were included in the fitting routine. Moreover, the addition of one or two new experimental lines to the data to be fitted often produced changes in both J and Q which were well beyond the standard deviations of the previous fit. This apparently random variation in the values of the isotropic interaction parameters was evidently *not* due to the relative insensitivity of the observed transitions to the J values, since this effect has already been included in the definition of the standard deviation. We must conclude, therefore, that there is some additional effect which correlates the J and Q values in the analysis.

To study this effect a number of fits were made in which J was held fixed at several different values while all other parameters, including the three $Q^{|m|}$, were allowed to vary. The result was quite

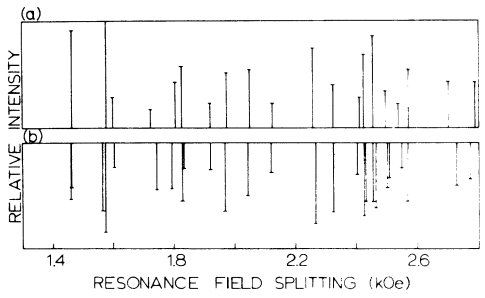

FIG. 14. Best fit to the nnn pair line splittings and intensities of Gd^{3+} in $Eu(OH)_3$. (a) Experimental spectrum at $T=77$K; (b) calculated spectrum using the parameters $g=1.990$, $J=-0.01460$ cm^{-1}, $\alpha=0.02531$ cm^{-1}, $b_2^0=0.00201$ cm^{-1}, $b_4^0=0.00002$ cm^{-1}, $b_6^0=-0.00003$ cm^{-1}.

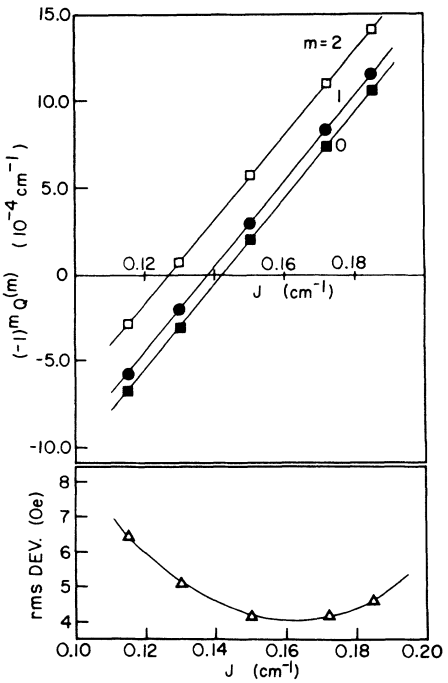

FIG. 15. Variation of the least-squares-fitted biquadratic parameters $(-1)^m Q^{|m|}$ and the rms deviation for different values of the bilinear exchange coefficient J.

striking. All the parameters other than the $Q^{|m|}$ varied very little, while the $Q^{|m|}$ increased significantly with J. Figure 15 shows the variation of the $Q^{|m|}$ for the case of the nn pairs in $Eu(OH)_3$, and also the corresponding rms deviations for different values of J. Several significant points were at once obvious from these results.

First, the rms deviation varied only from 4 to 7 Oe for J values ranging from 0.11 to 0.19 cm^{-1}. In view of the fact that the experimental resolution was approximately 7 Oe, it could only be concluded that corresponding sets of parameters with J anywhere within this range provide equally valid descriptions of the experimental spectrum. This is in marked contrast to the earlier results for the trichlorides (papers I and II), and also for the present results for the nnn, for which J was determined quite precisely by the over-all fit.

Secondly, all three biquadratic coefficients were *linear* functions of J *with identical values of the slope*, $(-1)^m\, dJ/dQ^{|m|} = 40.5 \pm 0.7$. The identical slopes immediately suggested that the biquadratic coefficients were absorbing components of some isotropic term, in order to compensate for the different values of J. This was confirmed by decomposing the values of $Q^{|m|}$ into a scalar part and an anisotropic part, according to Eqs. (5) and (6). It was then found that only the scalar coefficient Q varied with J, while the anisotropic coefficients $q^{|m|}$ were essentially independent of J. As would be expected from the variation of the individual $Q^{|m|}$, the dependence of Q on J was such that the combination $J - 40.5Q$ remained essentially constant.

Finally, the direct correlation between J and Q was evident in another way. The standard deviations for the $Q^{|m|}$ when all parameters were fitted were generally comparable to the parameter values themselves as indicated in Tables VII and IX. When the data were reprocessed with J fixed, the standard deviations decreased by an order of magnitude. It is apparent that the smaller values represent the appropriate limits for the anisotropic coefficients $q^{|m|}$, and these are the numbers listed in Table XII.

We thus concluded that the present analysis is able to determine the isotropic interactions only in form of the linear combination $J' = J - 41Q$, while the anisotropic terms are all determined individually and unambiguously by the fits to the spectra. The best estimates of J' are given in Table XII along with the corresponding values of the anisotropic parameters $q^{|m|}$.

To complete this analysis we still require an explanation for the origin of the slope $dJ/dQ = 41$. This can be understood by examining the particular transitions which are observed in the case of the nn spectra and used to determine the parameters. Since the dominant interactions in this case are isotropic, the only readily observable transitions are those between states which belong to the same multiplet of total spin, $\vec{T} = \vec{S}_1 + \vec{S}_2$. These states are perturbed and admixed by the anisotropic terms, and the strength of the isotropic interaction enters only through the energy differences between the

TABLE XII. Summary of spin-Hamiltonian parameters for Gd^{3+} pair interactions in $Y(OH)_3$ and $Eu(OH)_3$ at 77 K (in units of 10^{-4} cm^{-1}).

	$Y(OH)_3$		$Eu(OH)_3$	
	nn	nnn	nn	nnn
$J' = J - 41Q$	1640 ± 55	···[a]	1340 ± 71	···[a]
$q^{\|2\|}$	+2.7 ± 0.4	···	+1.9 ± 0.4	···
$q^{\|1\|}$	+1.4 ± 0.4	···	+0.9 ± 0.4	···
q^0	−2.6 ± 0.4	···	−2.0 ± 0.4	···
J	1640 ± 200[b]	−59.6 ± 1.0	1340 ± 200[b]	−146.0 ± 1.0
α	386.6 ± 1.0	260.6 ± 1.0	364.4 ± 0.9	252.7 ± 1.0
b_2^0	+1.0 ± 0.5	48.6 ± 0.2	−164.3 ± 0.5	20.0 ± 0.2
b_4^0	−2.0 ± 0.3	−0.9 ± 0.2	−2.0 ± 0.2	0.3 ± 0.2
b_6^0	+0.6 ± 0.1	−0.2 ± 0.2	+0.7 ± 0.2	−0.2 ± 0.2

[a]For the nnn J is determined independently of Q. (Q_{nnn} estimated $< 10^{-5}$ cm^{-1}.)

[b]J_{nn} estimated from J'_{nn} assuming $Q_{nn} = 0 \pm 5$ (10^{-4} cm^{-1}), as estimated from the comparison with the results in Ref. 6.

states which are admixed. In practice it turns out that only two energy differences are involved in the transitions which are observed: $\Delta E(T=0,\ T=2)$ and $\Delta E(T=1, T=3)$. This is because the anisotropic terms couple only states with $\Delta T=2$, and no transitions between states with $T>3$ are observed with the available sensitivity. These two energy differences are readily calculated in terms of J and Q, and one finds

$$\Delta E(T=0, T=2) = -3(J-42Q)$$

and

$$\Delta E(T=1, T=3) = -5(J-36Q).$$

It is now evident that the analysis of the spectra is not sensitive enough to distinguish between the two rather similar factors involved in these expressions, so that only an appropriate mean can be determined. It is not unreasonable that this mean should turn out to be $J-41Q$. In principle, one might of course try to distinguish between the two types of transitions and attempt to extract the two factors separately, and hence determine J and Q independently. However, in practice this will be very difficult when, as in the present case, Q is very much smaller than J (see below).

A much more promising way of determining J and Q independently would be to observe transitions which depended on $\Delta E(T, T\pm 2)$ directly, instead of relying on the weak second-order admixture. Unfortunately no such transitions could be found in spite of an intensive search, and we can only conclude that *inter*multiplet transitions are much weaker or broader than corresponding *intra*multiplet lines, for reasons which are not clear at this time.

At this point we must conclude therefore that the present EPR method is not able to separate the isotropic bilinear and biquadratic interactions for either of the nn pair spectra, although the linear combination $J'=J-41Q$ can be determined quite accurately. For the nnn pairs, on the other hand, the relatively weaker isotropic terms allow much larger admixtures by the anisotropic terms, which result in *inter*multiplet transitions which are sensitive to J and Q independently. In this case no evidence for a significant Q was found and J_{nnn} could be determined quite accurately.

2. *Comparison with* $Gd(OH)_3$ *Results*

Information about spin-spin interactions can also be obtained from analyses of bulk-susceptibility and specific-heat measurements, and in the present case this provides a useful upper limit on the so far elusive Q_{nn}. It can readily be shown that Q does not have any first-order effect on either the susceptibility or specific heat, and the second-order contributions proportional to $(Q)^2$ will be extremely small for all realistic values of Q. It is reasonable therefore to analyze the bulk properties ignoring Q and to estimate the interactions in terms of only the bilinear coefficients, J_{nn} and J_{nnn}. Such a analysis has recently been reported by Skjeltorp *et al.*,[6] who found in particular, for concentrated $Gd(OH)_3$, $J_{nn}[Gd(OH)_3] = 0.125 \pm 0.004\ cm^{-1}$.

This value may be compared with the two values of J'_{nn} determined by our resonance experiments (see Table XII), and it may be seen that the values for $Eu(OH)_3$ and $Gd(OH)_3$ agree quite closely. Inasmuch as these two lattices have identical structures with very similar dimensions (see Table I), it would seem reasonable to suppose that $J'_{nn}=J_{nn}-41Q_{nn}$ for $Gd(OH)_3$ would be within the range of J_{nn} values for the $Eu(OH)_3$ pair measurements listed above. Comparing these values with the bulk estimate of J_{nn}, we can conclude that $Q_{nn}[Gd(OH)_3]$ should be less than $\pm 5\times 10^{-4}\ cm^{-1}$, and it would seem likely that Q_{nn} for the pairs should be similarly small. Using these limits on Q_{nn} permits us to estimate the bilinear exchange as

$$J[Eu(OH)_3] = 0.134 \pm 0.020\ cm^{-1}$$

for $Eu(OH)_3$: Gd, and

$$J[Y(OH)_3] = 0.164 \pm 0.020\ cm^{-1}$$

for $Y(OH)_3$: Gd.

This estimate for Q_{nn} may be compared with the values of the anisotropic biquadratic coefficients $q^{|m|}$ which are listed in Table XII. It can be seen that the ranges of values are all quite similar, and we shall see later (Sec. VII A 3) that this is not unreasonable from a theoretical point of view. From a practical point of view we may note that all these terms are quite small on an absolute scale and since they produce no first-order effect on bulk properties, it is probably safe to ignore them for most thermodynamic calculations. However, for the detailed analysis of individual pair spectra, both isotropic and anisotropic biquadratic terms can and do make significant differences, and it certainly seems necessary to consider their possible contribution carefully in all such cases.

3. *Biquadratic Interaction Mechanisms*

There are two mechanisms which are commonly cited to account for biquadratic interaction terms. One is a second-order superexchange interaction, and this has been discussed by Anderson.[26] Its strength has been estimated to be of the order of J/U times the usual bilinear exchange, where U is the energy required to transfer an electron from one ion to a neighbor. U is generally of the order of a few eV and since $J\sim 0.1\ cm^{-1}$, this would here give $Q\sim 10^{-6}\ cm^{-1}$, a value which is quite consistent with our upper limit of $5\times 10^{-4}\ cm^{-1}$.

The second mechanism arises from exchange

striction and this has been found to contribute significantly to the biquadratic coupling in various $3d$ systems, such as MnO, [27] NiO, [27] Mn pairs in MgO[28,29] and CaO, [29] and Cr pairs in $ZnGaO_4$. [30] The strength of this mechanism is estimated to be

$$Q_{ES} \sim -\left(\frac{dJ}{dR}\right)^2 \Big/ 2cR,$$

where R is the ionic separation and c is an elastic stiffness constant. The rate of change of J with R for our kind of system may be estimated from earlier results for Gd^{3+} in different crystals, [7] which have been shown to be on an almost straight line with $dJ/dR \sim -0.15$ cm^{-1}/Å. Taking $c \sim 10^{12}$ dyn/cm^2, this gives $Q_{ES} \sim -0.5\times10^{-6}$ cm^{-1}. This is even smaller than our previous estimate, and we must conclude that neither of the commonly invoked mechanisms predicts any significant biquadratic interaction in the present case.

These estimates are quite consistent with our conclusion that the *isotropic* biquadratic terms are small, but they do nothing to explain the finite *anisotropic* terms which were necessary to fit the experimental data. Moreover, it is not possible to resolve this problem by increasing either of the above estimates, since both mechanisms can only give isotropic coupling terms, at least in the simple form in which they have been considered so far.

A simple extension of the exchange-striction mechanism, allowing for the effect of the separation dependence of the magnetic dipole interaction, has been considered previously in connection with the Gd^{3+} pair measurements in $LaCl_3$[4]. Such an extension might in fact account for the form of the observed anisotropy, but the absolute magnitude is again estimated to be about two orders of magnitude too small.

In a search for alternative interaction mechanisms we next considered electric quadrupole-quadrupole coupling between the Gd^{3+} ions. To a first approximation, the ground state of Gd^{3+} has no orbital angular momentum and thus no electric multipole moment. However, there are second-order admixtures due to spin-oribt coupling, and with these, weak electric interactions are permitted. The admixtures have been estimated by Wybourne, [31] who found an approximate ground state which may be written in the form

$$\left|J=\tfrac{7}{2}\right\rangle = 0.988\left|{}^8S_{7/2}\right\rangle + 0.162\left|{}^6P_{7/2}\right\rangle - 0.012\left|{}^6D_{7/2}\right\rangle. \tag{7}$$

To estimate the strength of the electric quadrupole-quadrupole (EQQ) coupling between a pair of ions described by states of this kind, we shall use a simple model of localized charges, neglecting for the moment complications from shielding and overlap. Following the notation of Wolf and Birgeneau[32] we write the EQQ interaction for a pair of neighbors in the form

$$V_{12} = \frac{(4\pi)^{3/2}e^2}{15\epsilon_0 R}\left(\frac{\langle r^2\rangle}{R^2}\right)^2 \times \sum_{i,j} B_m \sum_{i,j} Y_2^m(\theta_i,\phi_i) Y_2^{-m}(\theta_j,\phi_j), \tag{8}$$

where $B_m = 6$, 4, or 1 for $m = 0$, ±1, or ±2, and ϵ_0 is the effective dielectric constant which we shall set equal to 1 for the time being. Here R is again the ionic separation, $\langle r^2\rangle$ is the usual average over the $4f$ radial wave function, and the sum over i and j is over all electrons on ions 1 and 2. The required matrix elements of V_{12} thus reduce to sums of products of matrix elements of the form

$$\langle SLJJ_z \left| \sum_i Y_2^m(i) \right| S'L'J'J_z' \rangle ,$$

with $J = J' = \frac{7}{2}$ and $S = S'$, which may be evaluated readily using standard methods. [33] After some reduction, the final result, expressed in terms of the parameters $q^{|m|}$, could thus be estimated to be

$$q_{EQQ}^{|m|} \sim 0.01\left(\frac{\langle r^2\rangle}{R^2}\right)^2 B_m \text{ cm}^{-1}.$$

Taking $\langle r^2\rangle/R^2 \sim 0.03$, this gives $q^{|m|} \sim 10^{-5}$ cm^{-1}, which is about one order of magnitude smaller than the observed values. However, there are several factors in the present calculation which could well enhance the mechanism, and one can certainly not conclude that EQQ is inadequate for explaining the observed $q^{|m|}$. A discussion of the various complications which must be considered in a realistic calculation of the EQQ interaction has been given by Baker, [34] and it would seem clear that factors of 10 are well within the present range of uncertainty. Even the discrepancy between the relative sizes of the $q^{|m|}$ and the factors B_m could perhaps be removed by proper allowance for shielding and overlap.

However, for complete agreement, all these factors would have to combine in just the right way, and on balance it really does not seem very likely that EQQ coupling is in fact the principal interaction mechanism for the observed $q^{|m|}$.

An alternative mechanism, which we have rejected up to now by implication, is the possibility that the exchange interaction itself might have large anisotropic biquadratic terms, even though the isotropic terms are quite small. At first sight such an idea seems completely unlikely since one might guess that the anisotropic terms would be smaller than the isotropic terms by some factor of the order of $[(2-g)/g]^2$, as in the case of anisotropic bilinear exchange. [35] Such an estimate would then give

$$q^{|m|} \sim Q[(2-g)/g]^2 \lesssim 10^{-10} \text{ cm}^{-1},$$

which would clearly be quite negligible.

However, such a naive estimate fails to take into account the true form of anisotropic exchange and a more detailed analysis is required. Such a calculation has recently been carried out by Cone,[36] who considered the general form for the orbital dependence of the exchange as given by Levy,[37]

$$\mathcal{H} = \sum_{i,j} - \Gamma^{kk'}_{qq'} u^k_q(i) u^{k'}_{q'}(j) \{ \tfrac{1}{2} + 2\vec{S}_i \cdot \vec{S}_j \} , \qquad (9)$$

together with the admixtures of nonzero angular momentum states into the ground state [Eq. (7)].

Following a procedure similar to that mentioned above in connection with our own EQQ calculation and neglecting the small $^6D_{7/2}$ admixture, Cone was able to show that all of the $q^{|m|}$ could be expressed in terms of only *two* of the exchange parameters, Γ^{11}_{00} and $\Gamma^{1}_{1\pm1}{}^{1}$, and that all three were in fact proportional to the *same linear combination* $(\Gamma^{11}_{00} + \Gamma^{1}_{1-1}{}^{1})$. The relative magnitudes are thus uniquely predicted *independently of the* Γ's and evaluating the n-j symbols Cone found

$$q^{|2|} : q^{|1|} : q^0 = 2 : 1 : -2,$$

in striking agreement with the experimental values for both $Y(OH)_3$ and $Eu(OH)_3$, as shown in Table XII.

To calculate the absolute values one must estimate Γ^{11}_{00} and $\Gamma^{1}_{1-1}{}^{1}$ and this introduces some uncertainties. However, by combining recent analyses of optical measurements[38] on $Gd(OH)_3$ and $GdCl_3$, Cone was able to make reasonable estimates for the Γ's which led to q's within a factor of 5 ± 3 of our observed values. Details of this analysis and a discussion of the uncertainties will be given elsewhere,[36] but we can already conclude here that a proper calculation of the effect of orbital anisotropy in the usual (bilinear) exchange seems to account for both the qualitative and quantitative aspects of our small biquadratic terms.

This result has a number of other implications, both for our particular systems as well as for other situations in which isotropic bilinear (Heisenberg) exchange has previously been considered to be dominant.

First, it is clear that the inclusion of states other than the ^6P in the admixture will permit contributions from higher-rank tensors in the general interaction [Eq. (9)], and these in turn will result in higher-degree terms in the effective spin-spin interactions. In the present case these may be expected to be quite small, since the amplitude of the $^6D_{7/2}$ state is relatively small [Eq. (7)], and indeed we were able to obtain a satisfactory fit to the observed spectra without having to include any such terms. However, in other cases we can certainly expect larger admixtures of states with $L > 1$ into the ground state, and we should then find correspondingly larger high-rank interactions of the form $O^{(k)}_q(S_1) O^{(k')}_{q'}(S_2)$ with k and $k' > 2$.

The second implication of these cross-term effects is a prediction of a contribution to the isotropic biquadratic coupling in the ground state. This is simply a consequence of the recoupling of terms of the form of Eq. (9) to give a second-rank contribution, which in general will certainly have an isotropic part as well as anisotropic part. Indeed, in general one might expect both parts to be comparable in magnitude, and in the present case this would correspond to a $Q \sim 10^{-4}$ cm^{-1}. This is still well inside the upper limit estimated from the data, but it is interesting to note that it is about two orders of magnitude *larger* than the values estimated on the basis of Anderson's[26] second-order superexchange. It could well be that a similar effect could account for some of the anomalously large biquadratic exchange terms observed in other systems.[27-30]

A more detailed discussion of these effects is clearly beyond the scope of the present paper, and we need here note only that the anisotropic biquadratic terms which we were forced to include empirically to fit our data are by no means unreasonable, and that their presence may indeed imply a number of other new effects both in these systems and in others.

B. Bilinear Interaction Terms

We have given a rather extensive discussion of the biquadratic terms because their effects are new, but from an over-all point of view the more usual bilinear terms are still much more important. From Table XII we can see that by far the largest interaction is the nearest-neighbor J_{nn}, with J_{nnn} and the magnetic dipole interactions for both the nn and nnn smaller but still significant. As noted previously, the dipole parameters are in excellent agreement with the calculated values (see Table I), confirming both the analysis and the absence of large anisotropic bilinear exchange terms.

The observed values of J, on the other hand, are much more difficult to explain. Not only their relative magnitudes but even their signs are not predicted by any microscopic theory, and this remains as a challenge to all first-principles theories of exchange interactions.

From a purely phenomenological point of view we may note that all four J values are consistent with a previously noted[7] trend of J with R, which would seem to indicate *that superexchange via the ligands may not be the most important mechanism* in systems of this kind. It is not clear whether the dominant interaction is via the closed $5s5p$ shells or some other form of overlap, but it would appear that the exchange coupling in these materi-

als is the result of quite a complex competition between several factors.

Considering the J values as purely empirical quantities, it is immediately obvious from Table XII why $Gd(OH)_3$ behaves so differently from the apparently similar $GdCl_3$. First, we see that the dominant interaction is antiferromagnetic in sign, in contrast to the dominant ferromagnetic J_{nnn} in $GdCl_3$. This explains the striking difference in the cooperative properties. Second, we may note that the dominant interactions are here between nearest neighbors along one-dimensional linear chains, which in the absence of other interactions would not order at all. Long-range order thus depends critically on the much weaker interactions between chains, and this explains the fact that the ordering temperature is relatively low, in spite of the expected stronger interactions.

The detailed cooperative behavior is further complicated by unusual cancellations produced by the high symmetry of the hydroxide structure. These have been discussed by Skjeltorp *et al.*,[6] and it is evident that a number of interesting questions remain to be explained.

C. Crystal Field Terms

The crystal field parameters required to fit the spectra are also given in Table XII. Comparison with the single-ion parameters reveals two interesting features. First, in all cases, by far the largest term is b_2^0, which varies from system to system, while b_4^0 and b_6^0 remain small and much more constant. Second, the shifts between the single-ion values for b_2^0 and the corresponding pair values show an interesting systematic trend. Empirically, these shifts are

$$\Delta b_2^0[\text{nn } Y(OH)_3 : Gd] = +0.0131 \text{ cm}^{-1},$$

$$\Delta b_2^0[\text{nnn } Y(OH)_3 : Gd] = +0.0021 \text{ cm}^{-1},$$

$$\Delta b_2^0[\text{nn } Eu(OH)_3 : Gd)] = -0.0023 \text{ cm}^{-1},$$

$$\Delta b_2^0[\text{nnn } Eu(OH)_3 : Gd] = -0.0010 \text{ cm}^{-1},$$

where we have written $\Delta b_2^0 = b_2^0(\text{pair}) - b_2^0(\text{ion})$. Since even the origin of the single-ion parameters remains an unresolved question, there is clearly no hope of explaining these shifts at this time, but it is interesting to note that the *signs* of Δb_2^0 follow a simple pattern. Whenever Gd^{3+} is doped into a host of larger dimension than the isomorphic Gd salt, Δb_2^0 is negative and *vice versa*. Such a correlation also describes the earlier results for Gd^{3+} in $LaCl_3$[4], $EuCl_3$[5], and lanthanum ethyl sulphate,[39] and it would thus appear to have some general validity. However, it is not clear whether any more quantitative analysis can be made along this line, and for the present we must regard the b_2^0 as purely empirical parameters which must be determined in each case.

D. Gd^{3+}-Eu^{3+} Interactions

In addition to providing information about Gd^{3+}-Gd^{3+} interactions, the measurements on Gd^{3+} single ions and pairs in $Eu(OH)_3$ also provide estimates of the Gd^{3+}-Eu^{3+} interactions. The analysis is identical to that previously employed for Gd^{3+} in $EuCl_3$[5], and we can immediately take over Eqs. (7a) and (8b) given in II to solve for J_{nn} and J_{nnn} in terms of the observed g shifts (see Sec. IV). Substituting, we find

$$J_{nn}(Gd^{3+}\text{-}Eu^{3+}) = 0.06 \pm 0.09 \text{ cm}^{-1}$$

and

$$J_{nnn}(Gd^{3+}\text{-}Eu^{3+}) = -0.005 \pm 0.050 \text{ cm}^{-1}.$$

The large uncertainties in these values prohibit any strong quantitative conclusions, but it is interesting to note the qualitative similarity of both these results to the corresponding Gd^{3+}-Gd^{3+} interactions (see Table XII). As in the previously studied case of $EuCl_3$[5]: Gd, it would thus appear that the average electron-electron exchange interaction is roughly the same for both the $4f^8$ and $4f^7$ configurations, as suggested by Van Vleck.[40]

VIII. SUMMARY AND CONCLUSIONS

In this paper we have presented EPR measurements on single-ion and pair spectra of Gd^{3+} in two rare-earth hydroxides, $Y(OH)_3$ and $Eu(OH)_3$. The data were analyzed following the earlier work on Gd^{3+} in $LaCl_3$ and $EuCl_3$, and generally similar results were obtained. However, a number of unexpected effects were observed, which are of some interest.

For the nearest-neighbor pairs it was found that the resonance method could not readily distinguish between isotropic bilinear (Heisenberg) and biquadratic interactions, and only the linear combination $J_{nn} - 41\,Q_{nn}$ could be determined with accuracy. Comparison with an analysis of bulk properties of concentrated $Gd(OH)_3$ allowed an upper limit to be set on Q_{nn} ($Q_{nn} < 5\times10^{-4}$ cm^{-1}), and it was finally concluded that isotropic biquadratic interactions are in fact relatively unimportant in these materials.

At the same time it was found that *anisotropic* biquadratic interactions of a similar magnitude are by no means negligible in the explanation of the observed spectra, and accurate values of the three parameters characterizing the axially symmetric components were determined. Such interactions have relatively little influence on observable bulk properties, but they can be quite important for the detailed analysis of precise spectral information.

For the next nearest neighbor, no influence of

biquadratic interactions was detected, and the spectra could be fitted in terms of the usual bilinear exchange and magnetic dipole coupling.

Crystal field terms were found to be quite important for both the nn and nnn pairs, and, in particular, b_2^0 was found to be relatively large and different for the various kinds of pairs. However, on an absolute scale, the crystal field contributions were really quite small, as previously found in the isostructural trichlorides.

The parameters describing the anisotropic bilinear interactions were found in all cases to be equal to the values calculated on the basis of magnetic dipole-dipole coupling, and we may conclude that anisotropic bilinear exchange is zero within the experimental limits.

The results have thus shown that the significant interactions for both nearest and next nearest neighbors are characterized by a single parameter J, as we would expect for pairs of Gd^{3+} ions. Values of J were extracted from the detailed analysis, and the results are given in Table XII, which includes also values for all the other parameters used to fit the spectra.

Examination of the J values shows both qualitative similarities and quantitative differences from the earlier results for Gd^{3+} in $LaCl_3$ and $EuCl_3$. For all four systems the nearest-neighbor interaction is found to be *antiferromagnetic* in sign, while the next-nearest-neighbor interaction is *ferromagnetic*. However, in the hydroxide case it is the nearest-neighbor coupling which is dominant in strength, while for the trichlorides the next-nearest-neighbor interactions are strongest. This explains at least empirically the previously surprising difference between $Gd(OH)_3$ and $GdCl_3$.

The observed J values are consistent with a systematic trend previously noted for several other Gd^{3+} systems, and it would seem that exchange parameters can now be predicted using these purely empirical results.

At the same time there is apparently no microscopic explanation for either magnitudes or even the signs of the observed J's, or indeed for most of the other parameters used to fit the spectra. A discussion of the biquadratic terms showed that the small isotropic component (Q) is not unreasonable, and that the anisotropic components $q^{|m|}$ are most probably due to the orbital dependence of the exchange acting through the spin-orbit admixture of nonzero angular momentum states into the ground state. Also there appears to be some correlation between the crystal field parameters b_2^0 and the size of the crystal host lattice, but only qualitative predictions seem possible at this time.

We must conclude, therefore, that the empirical determination of all the spin-Hamiltonian parameters is still far more accurate than any of the attempts to account for them theoretically, and it would seem most useful to use them mainly for correlating different experimental results. In this connection we may note that the comparison between the susceptibility and specific-heat results for $Gd(OH)_3$ and the present pair measurements has provided a very satisfactory over-all description of this system, even though no "first principles" estimates of the principal interactions can be made. In the long run, however, a detailed comparison between the empirical parameters and microscopic calculations would be most desirable, and this remains as a clearly defined challenge to the theory of exchange and electric multipole interactions.

ACKNOWLEDGMENTS

We are extremely grateful to S. Mroczkowski and J. Eckert for providing the crystals used in these experiments. We would also like to thank R. J. Birgeneau for the use of a number of his fitting programs, C. A. Catanese, H. E. Meissner, and A. T. Skjeltorp for making available to us their susceptibility and specific-heat data on $Gd(OH)_3$, and R. L. Cone for informing us about his anisotropic exchange calculations prior to publication. We are pleased to acknowledge many helpful discussions with the above and also with M. F. Thorpe and R. A. Alben. One of us (R. W. C.) would like to thank the National Research Council of Canada for the award of a postdoctoral fellowship during this work, and one of us (W. P. W.) would like to thank the Physics Department of Brookhaven National Laboratory for their gracious hospitality during the preparation of the final manuscript.

---

*Supported in part by the U.S. Atomic Energy Commission and in part by the National Science Foundation.

†National Research Council of Canada Postdoctoral Fellow. Present address: Eaton Electronics Research Laboratory, McGill University, Montreal 101, P.Q. Canada.

‡Present address: Dept. of Electrical Engineering, University of Singapore, Singapore 2.

[1]W. P. Wolf, H. E. Meissner, and C. A. Catanese, J. Appl. Phys. **39**, 1134 (1968).

[2]W. P. Wolf, H. E. Meissner, C. A. Catanese, and P. D. Scott, Colloq. Int. Cent. Natl. Rech. Sci. **180**, 93 (1970).

[3]W. P. Wolf, M. J. M. Leask, B. Mangum, and A. F. G. Wyatt, J. Phys. Soc. Jap. Suppl. **17**, 487 (1961).

[4]M. T. Hutchings, R. J. Birgeneau, and W. P. Wolf, Phys. Rev. **168**, 1026 (1968).

[5]R. J. Birgeneau, M. T. Hutchings, and W. P. Wolf, Phys. Rev. **179**, 275 (1969).

[6]A. T. Skjeltorp, C. A. Catanese, H. E. Meissner, and W. P. Wolf,

Phys. Rev. B **7**, 2062 (1973).
[7]R. W. Cochrane and W. P. Wolf, Solid State Commun. **9**, 1997 (1971).
[8]See, for example, M. T. Hutchings, in *Solid State Physics*, edited by F. Seitz and D. Turnbull (Academic, New York, 1964), Vol. 16, p. 227.
[9]It seems quite reasonable to consider biquadratic terms before other higher-order functions since all of the physically likely mechanisms would produce perturbations whose lowest-order effect would be biquadratic in the spin operators.
[10]D. Smith and J. H. M. Thornley, Proc. Phys. Soc. Lond. **89**, 779 (1966).
[11]The normalized spherical tensors $O_q^{(k)}$ used in these terms are related through normalizing factors to the more conventional crystal-field operators used in Eq. (2). See also H. A. Buckmaster, Can. J. Phys. **40**, 1670 (1962); and R. J. Birgeneau, Can. J. Phys. **45**, 3761 (1967).
[12]By choosing normalized spherical tensors for the definition of $\mathcal{H}_Q(1, 2)$, one can readily extract the scalar invariant using standard recoupling methods. [See, for example, A. R. Edmonds, *Angular Momentum in Quantum Mechanics* (Princeton U. P., Princeton, N.J., 1960), Chap. 5, p. 68.] The required vector coupling coefficients $(2m\,2 - m \mid 2200)$ are here identically equal to the corresponding 3-j symbols (Edmonds, p. 46)

$$\begin{pmatrix} 2 & 2 & 0 \\ m & -m & 0 \end{pmatrix} = (-1)^m \frac{1}{\sqrt{5}}$$

The scalar invariant of Eq. (4) may also be written in the more usual but less convenient form

$$\mathcal{H}_{QS}(1,\ 2) = Q[\tfrac{3}{2}(\vec{\mathrm{S}}_1 \cdot \vec{\mathrm{S}}_2)^2 + \tfrac{3}{4}(\vec{\mathrm{S}}_1 \cdot \vec{\mathrm{S}}_2) - \tfrac{1}{2} S^2(S+1)^2].$$

[13]R. Fricke and A. Seitz, Z. Anorg. Allg. Chem. **254**, 107 (1947).
[14]S. Mroczkowski, J. Eckert, H. Meissner, and J. C. Doran, J. Cryst. Growth **7**, 333 (1970).
[15]P. V. Klevtsov and L. P. Sheina, Neorg. Materialy **1**, 912 (1965).
[16]R. J. Birgeneau, Ph.D. thesis (Yale University, 1967) (unpublished).
[17]C. P. Poole, Jr., *Electron Spin Resonance* (Interscience, New York, 1967).
[18]We are grateful to Professor A. Brill of the University of Virginia for supplying us with some of this material.
[19]P. D. Scott, J. Chem. Phys. **54**, 5384 (1971).
[20]B. Bleaney, H. E. D. Scovil, and R. S. Trenam, Proc. R. Soc. A **223**, 15 (1954).
[21]M. T. Hutchings, C. G. Windsor, and W. P. Wolf, Phys. Rev. **148**, 444 (1966).
[22]M. J. D. Powell, J. Comput. Phys. **7**, 303 (1965).
[23]See, for example, Y. V. Linnik, *Method of Least Squares and Principles of the Theory of Observations* (Pergamon, New York, 1961).
[24]R. W. Cochrane, C. Y. Wu, and W. P. Wolf, J. Appl. Phys. **42**, 1568 (1971).
[25]The rms deviation of 9 Oe for the nnn compared to the much larger value for the nn ($\sim$ 30 Oe) without biquadratic terms implies that the biquadratic coefficients must be at least an order of magnitude smaller than the nn coefficients, i.e., $Q_{\mathrm{nnn}}^{|m|} \leq 10^{-5}$ cm^{-1}. This is consistent with the estimate of the order of magnitudes of possible biquadratic terms discussed in Sec. VII A.
[26]P. W. Anderson, in *Solid State Physics*, edited by F. Seitz and D. Turnbull (Academic, New York, 1963), Vol. 14, p. 99.
[27]D. S. Rodbell and J. Owen, J. Appl. Phys. **35**, 1002 (1964).
[28]E. A. Harris and J. Owen, Phys. Rev. Lett. **11**, 9 (1963); D. S. Rodbell, I. S. Jacobs, J. Owen, and E. A. Harris, Phys. Rev. Lett. **11**, 10 (1963).
[29]E. A. Harris, J. Phys. C **5**, 338 (1972).
[30]J. C. M. Henning and J. P. M. Damen, Phys. Rev. B **3**, 3852 (1971); J. C. M. Henning, J. H. Den Boef, and G. G. P. van Gorkom, Phys. Rev. B **7**, 1825 (1973).
[31]B. G. Wybourne, Phys. Rev. **148**, 317 (1966).
[32]W. P. Wolf and R. J. Birgeneau, Phys. Rev. **166**, 376 (1968).
[33]The appropriate reduced matrix elements and 3-j symbols have been tabulated by C. W. Nielson and G. Koster [*Spectroscopic Coefficients for p^n, d^n and f^n Configurations* (M.I.T. Press, Cambridge, Mass., 1964)] and M. Rotenberg, R. Bivins, N. Metropolis, and J. K. Wooten, Jr. [*The 3-j and 6-j Symbols* (Technology, Cambridge, Mass., 1959)].
[34]J. M. Baker, Rep. Prog. Phys. **34**, 109 (1971).
[35]J. H. Van Vleck, Phys. Rev. **52**, 1178 (1937).
[36]R. L. Cone (unpublished).
[37]P. M. Levy, Phys. Rev. **177**, 509 (1969).
[38]R. L. Cone and R. S. Meltzer, Phys. Rev. Lett. **30**, 859 (1973).
[39]R. J. Richardson and S. Lee, Phys. Rev. B **1**, 108 (1970).
[40]J. H. Van Vleck, Rev. Univ. Nac. Tucuman A **14**, 189 (1962).